

©Copyright 2010 DigiPen Institute of Technology and DigiPen (USA)  
Corporation. All rights reserved.

# Non-Photorealistic Real-Time Edge Rendering using Non-Duplicate Parallel Detection and Capping

BY  
Dwight House  
B.S. Computer Science, Louisiana State University Shreveport, 2007

## *THESIS*

Submitted in partial fulfillment of the requirements  
for the degree of Master of Science  
in the graduate studies program  
of DigiPen Institute of Technology  
Redmond, Washington  
United States of America

Summer  
2010

Thesis Advisor: Dr. Xin Li

DIGIPEN INSTITUTE OF TECHNOLOGY  
GRADUATE STUDY PROGRAM  
DEFENSE OF THESIS

THE UNDERSIGNED VERIFY THAT THE FINAL ORAL DEFENSE OF THE  
MASTER OF SCIENCE THESIS OF Dwight House

HAS BEEN SUCCESSFULLY COMPLETED ON May 21st, 2010

TITLE OF THESIS: Non-Photorealistic Real-Time Edge Rendering using  
Non-Duplicate Parallel Detection and Capping

MAJOR FIELD OF STUDY: COMPUTER SCIENCE.

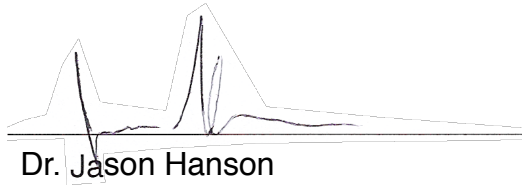
COMMITTEE:



Dr. Xin Li, Chair



Dr. Gary Herron



Dr. Jason Hanson



Mr. Chris Peters

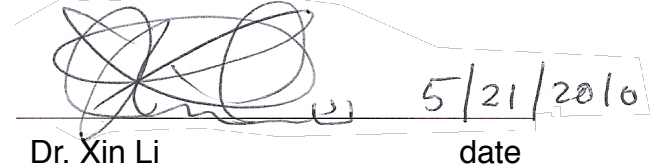
APPROVED:



5/21/2010  
date

Dr. Xin Li

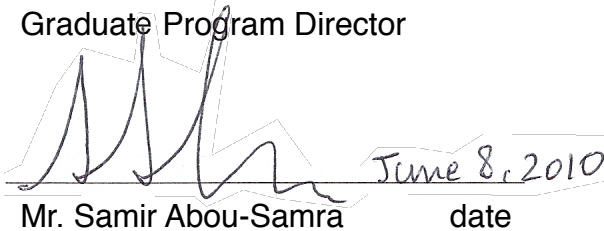
Graduate Program Director



5/21/2010  
date

Dr. Xin Li

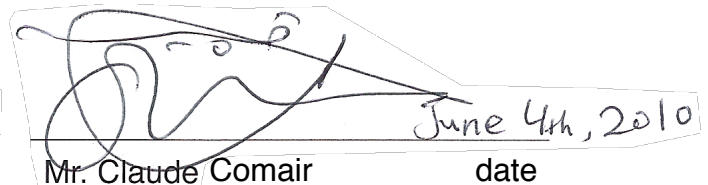
Dean of Faculty



June 8, 2010  
date

Mr. Samir Abou-Samra

Department of Computer Science



June 4th, 2010  
date

Mr. Claude Comair

President

The material presented within this document does not necessarily reflect the opinion of the Committee, the Graduate Study Program, or DigiPen Institute of Technology.

**INSTITUTE OF DIGIPEN INSTITUTE OF TECHNOLOGY**  
**PROGRAM OF MASTER'S DEGREE**  
*THESIS APPROVAL*

*DATE:* \_\_\_\_\_ May 21st, 2010 \_\_\_\_\_

BASED ON THE CANDIDATE'S SUCCESSFUL ORAL DEFENSE, IT IS  
RECOMMENDED THAT THE THESIS PREPARED BY

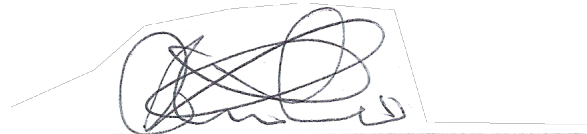
Dwight House

ENTITLED

Non-Photorealistic Real-Time Edge Rendering using Non-Duplicate

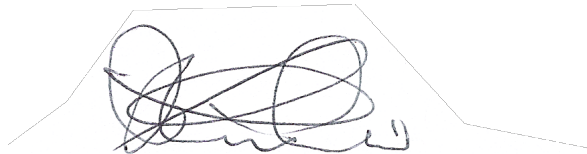
Parallel Detection and Capping

BE ACCEPTED IN PARTIAL FULFILLMENT OF THE REQUIREMENTS FOR  
THE DEGREE OF MASTER OF COMPUTER SCIENCE FROM THE PROGRAM  
OF MASTER'S DEGREE AT DIGIPEN INSTITUTE OF TECHNOLOGY.



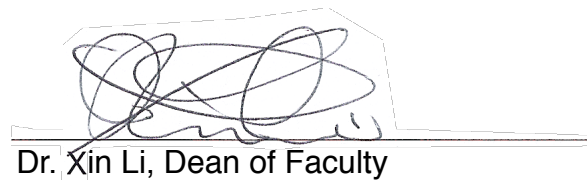
Dr. Xin Li

Thesis Advisory Committee Chair



Dr. Xin Li

Director of Graduate Study Program



Dr. Xin Li, Dean of Faculty

The material presented within this document does not necessarily reflect the opinion of the Committee, the Graduate Study Program, or DigiPen Institute of Technology.

## Acknowledgements

---

I would like to thank my family for their unending love, support, and encouragement. I thank also my friends who gave me moral support and assistance throughout the creation of this thesis. Thanks to Dr. Herron for his assistance in several key areas of my thesis study. Finally, I thank my thesis advisor Dr. Li for his guidance, patience, and kind words.

# Table of Contents

---

<b>1. Abstract</b>	<b>1</b>
.....	
<b>2. Introduction</b>	<b>2</b>
.....	
2.1. Applications of Edge Detection	4
.....	
2.2. Types of Edges	5
.....	
<b>3. Edge Detection Method Overview</b>	<b>8</b>
.....	
<b>4. Hardware Methods</b>	<b>9</b>
.....	
4.1. Back-Facing Wireframe Contours	9
.....	
4.2. Back-Facing Filled Polygon Contours	11
.....	
4.3. Offset Back-Facing Filled Polygon Contours	11
.....	
4.4. Thickness-Normalized Back-Facing Filled Polygon Contours	13
.....	
4.5. Stencil-Based Pixel Shifted Silhouettes	14
.....	
4.6. Inverted Stencil Contours	16
.....	
4.7. Hardware Creases and Contours	17
.....	
<b>5. Image-Space Methods</b>	<b>19</b>
.....	
5.1. Image Processing with the Sobel Operator	19
.....	
5.2. Other Operators	20
.....	
5.3. Input Imagery	22
.....	
5.4. Modern Implementation	23
.....	
5.5. Technique Variations	25
.....	
5.6. Advantages and Disadvantages	25
.....	
<b>6. Object-Space Methods</b>	<b>27</b>
.....	
6.1. Drawable Edge Tests	27
.....	
6.2. Edge Detection	29
.....	
6.3. Edge Rendering	32
.....	

6.4. Thick Edge Gaps	34
<b>7. Miscellaneous Methods</b>	<b>36</b>
7.1 Surface Angle Contours	36
7.2 Expanded Inverted Geometry Contours	37
<b>8. Morgan McGuire and John F. Hughes' Hardware-Determined Feature Edges</b>	<b>38</b>
8.1. Data Structure	38
8.2. Edge Detection	40
8.3. Edge Creation	41
8.4. Cap Creation	44
8.5. Problems	46
<b>9. Miscellaneous Contributions</b>	<b>47</b>
9.1. Depth-Based Edge Thickness	47
9.2. Reduce Effects of Incorrectly Projected Normals	51
9.3. Alternate Drawable Edge Types	54
<b>10. Non-Duplicate Parallel Edge Detection and Capping</b>	<b>58</b>
10.1. Method Overview	58
10.2. Data Structure	59
10.3. OpenCL Notes	61
10.4. Edge Detection and Creation	62
10.5. Cap Detection and Creation	63
10.6. Rendering	66
<b>11. Comparative Analysis</b>	<b>68</b>
11.1. Operation Quantities	69
11.2. Memory	72

11.3. Rendered Output	77
11.4. Speed	77
<b>12. Conclusion</b>	<b>81</b>
<b>13. Future Work</b>	<b>82</b>
<b>Work Cited</b>	<b>84</b>
<b>Bibliography</b>	<b>87</b>

# 1. Abstract

---

Non-photorealistic rendering (NPR) provides distinctly different information to the viewer when compared with photorealistic rendering. Examples of NPR range from visually pleasing toon and watercolor styles to the highly precise and informative technical illustration styles. One of the most important structures that can be found in many different NPR styles is the humble edge. It can define boundaries, amplify structure, highlight importance, and is an essential component of several artistic styles. Their utility has inspired research on real-time edge detection and rendering techniques since the early days of computer graphics. There are dozens of diverse methods to achieve real-time edge detection and rendering.

In this thesis, a survey of major edge detection methods is presented. The methods in the survey are divided into four distinct categories. Next, Morgan McGuire and John F. Hughes' "Hardware-Determined Edge Features" method is described in detail. It forms the basis for the author's exploration of, and contributions to, edge detection. Then, the author details his attempts to correct the problems with McGuire and Hughes' method. A few alternative methods are explored that take advantage of OpenCL, a new GPU computation technology. Finally, the effectiveness of the contributions are analyzed and compared.

## 2. Introduction

---

Non-photorealistic rendering (NPR) is any rendering with an intent other than the creation of photorealistic imagery. The power and customizability of more recent graphics card hardware has made real-time NPR a reality in popular media and games. One structure that spans nearly all forms of non-photorealistic rendering is the humble edge. Edges have surprising expressive power for their relative simplicity. Using edges, inner-object structure and the differentiation of nearby objects can be amplified and stylized. The following images are some examples of games that use edges and other effects in their non-photorealistic rendering.



*Figure 2-1: Viewtiful Joe (Capcom Production Studio 4) uses edge detection, cell shading, and various movie and anime-inspired animation effects to achieve an over-the-top graphical experience to match the chaotic nature of the gameplay. (Image courtesy of The Next Level [Next Level, The 03])*



*Figure 2-2: Ōkami (Ready at Dawn) makes use of a simpler, more sketchy edge detection along with screen-space canvas texturing and blurred cell-shading to create the visual appearance of a painting. (Image courtesy of Binge Gamer [Binge Gamer 08])*

There are many methods of detecting and rendering edges. The author has chosen to limit the topic only to real-time edge detection on polygonal meshes. The author also focuses on the detection of edges over their subsequent rendering. Even with these restrictions, dozens of methods and considerations remain.

The practical applications of edges are detailed and the edge types are defined in the remainder of the introduction. Next, a survey of edge detection and rendering methods is presented. The various methods are broken down into four sub-categories: hardware, image-space, object-space, and miscellaneous methods. Then, a paper by Morgan McGuire and John F. Hughes on GPU accelerated edge detection is described in detail as it forms the basis the author's research. The author then explains his research and contributions, including attempts to address failures, and exploration of alternative, but similar, edge detection methods. These new variations are analyzed and compared to McGuire and Hughes' method in terms of speed, memory usage, and overall calculation quantity. Finally, the author suggests additional possibilities for improvement.



*Figure 2-3: Several Utah Teapots rendered with depth-scaled object-space edge detection and a normal shader.*

## 2.1. Applications of Edge Detection

Edge detection and rendering are used primarily for graphical styles and to provide structural and positional differentiation. A list of known edge applications is below.

- **Differentiate objects** - An outer border on an object can differentiate it from other objects and the rest of the scene in the absence of shading. With shading, it enhances the contrast between objects.
- **Differentiate sections of objects** - An edge can serve to divide up various sections of a single object. For example, edges outlining a character's clothes will greatly differentiate the clothes from the character's skin and face.
- **Enhance structural perception** - Within the object, the edges can give a greater weight to a specific part of the mesh, such as the nose or eyes of a face. Without shading, edges are fully capable of expressing the basic structure to the mesh.
- **Highlighting** - If one object needs to be in focus, edges on the object can help differentiate it from all other objects.
- **Anti-Aliasing** - Rendering systems typically blend colors and textures across the surface of the polygon meshes, but on the edges of these meshes, aliasing occurs because at any given time, the renderer does not know what the neighboring pixels should be. Edge detection allows a focused application

of a blur, which significantly reduces the aliasing artifacts. This is a common method of anti-aliasing when using deferred shading.

- **Achieve specific graphical styles** - A wide variety of visual styles require edge detection as one of their major components. Such visual styles include: toon shading, technical and architectural illustration, pencil/pen styles, some forms of fur rendering, and several others.

## 2.2. Types of Edges

There are only a handful of edge types, but the terminology varies from book to book and paper to paper. For this thesis, the author will mention the variations in wording in the title of the types below, but will use the first mentioned name as the standard term for each type. Additionally, for the purposes of this thesis, all models and edges are described in terms of polygons. Edge detection and rendering for non-polygon objects is beyond the scope of this thesis.

### ***Contour/Silhouette/Outline Edge***

Contour edges are the polygon edges for which one adjacent polygon is front-facing and the other is back-facing. Contours are view-dependent and animation dependent. They cannot be pre-calculated, though some methods can use preprocessing to increase the speed of the test.

There is often need to differentiate the outer contour that surrounds the object from internal contours. Some visual styles prefer to have a thicker edge on the outer contours in order to reinforce the difference between each object. In this paper, the author chooses to call this subtype “silhouette.” There is a lot of terminological conflict over this type of edge. Many papers refer to all contours, internal and external, as silhouettes.

### ***Crease/Hard/Feature Edge***

Crease edges represent discontinuities in the surface of a mesh. A polygon edge is a crease edge if the angle between the adjacent polygons’ normals is greater than a user-defined “dihedral” angle [Gooch and Gooch 01]. Some implementations choose to split crease edges into two sub-categories, ridge and valley creases [McGuire and Hughes 04].

- **Ridge Crease Edge** - A crease edge where the internal angle between the two adjacent polygons is less than a user-defined ridge dihedral angle.
- **Valley Crease Edge** - A crease edge where the external angle between the two adjacent polygons is less than a user-defined valley dihedral angle.

Crease edges are not view dependent, but they can change based on animation.

### ***Boundary/Border/Surface Boundary Edge***

Boundary edges only occur on non-closed models [Gooch and Gooch 01]. It is a polygonal edge of only one polygon. These edges are not view-dependent and do not change with animation. Thus, they can be pre-calculated with no ill effects.

### ***Intersection/Self-Intersection/Collision Edge***

Intersection edges occur when two polygon surfaces pass through each other such that their intersection line does not correspond to a polygon edge. This is the least mentioned edge type in the literature. Some papers ignore these edges and others define them as self-intersections, only applying them to meshes that pass through themselves. No paper the author has read has accounted for these types of edges formed by the intersection of polygons from two different meshes, though the concept is identical. Self-intersection edges may be pre-calculated as long as they do not animate. Intersection edges between different objects can only be pre-calculated if both objects do not animate or move relative to each other.

### ***Marked/Material Edge***

Marked edges are merely polygon edges that the user has defined to always be a drawn edge. These edges are not view-dependent or animation-dependent, because they are pre-calculated by definition. Often they are used to separate major sections of a mesh regardless of orientation.

### ***Drawable Edge***

This is the author's term for the polygon edges that will be drawn on a given frame, as opposed to all those that are not drawn. It can be used to refer to any other type of edge, except intersection edges. This differentiation is used to avoid ambiguity when discussing object-space edge detection.

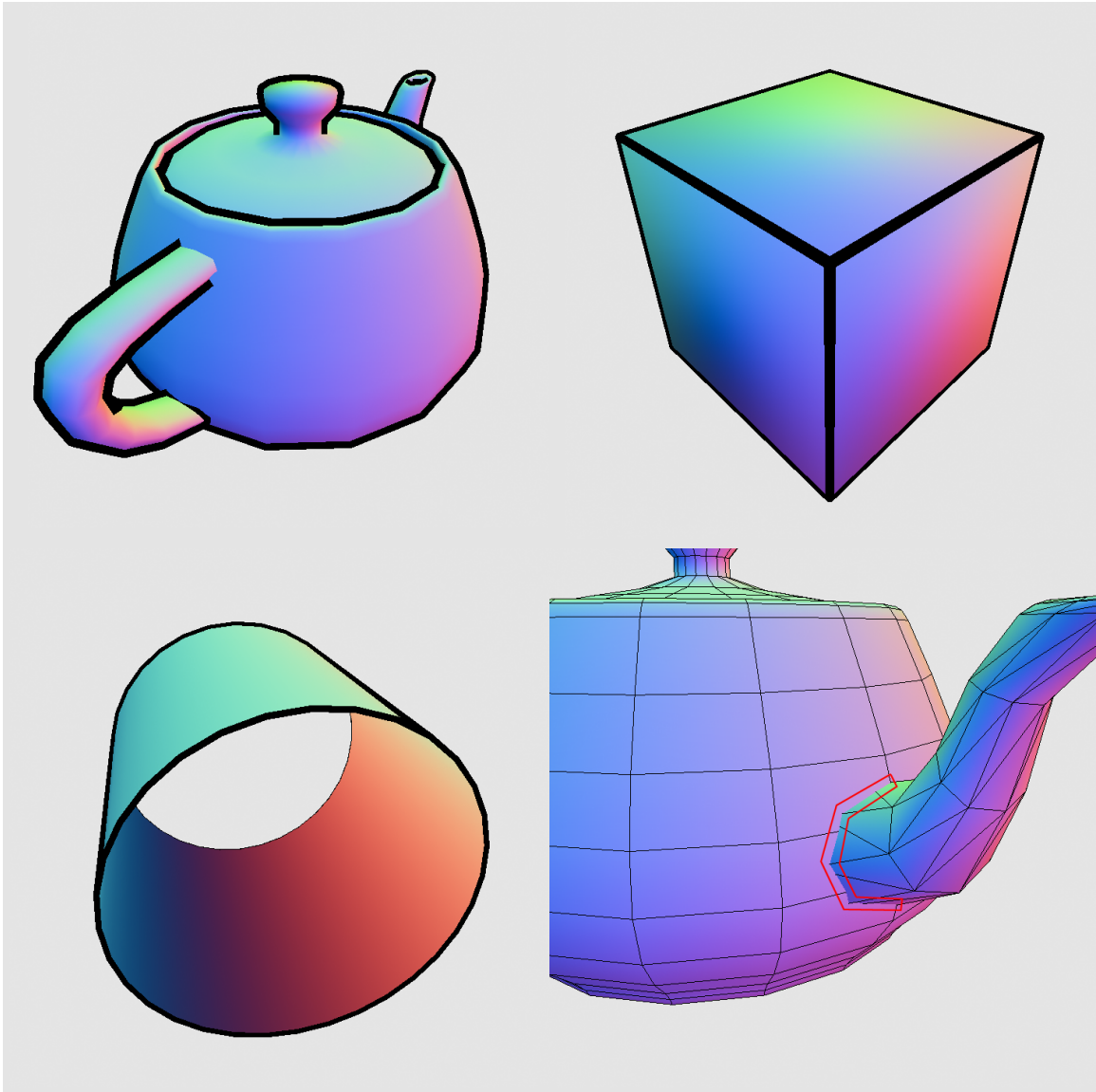


Figure 2-4: The teapot on the top-left shows contour edges. Notice how contour edges can be internal and external (silhouettes). The cube on the top-right is made up of creases (inner edges) and silhouettes (outer edges). The edges on the two ends of the tube on the bottom-left are boundary edges. The bottom-right image shows that the polygons of the teapot do not correspond to the intersection edge highlighted in red.

### **3. Edge Detection Method Overview**

---

There are dozens of ways to detect and render edges in real-time. They all fit into roughly four categories: hardware, image-space, object-space, and miscellaneous methods. Hardware methods are quick and simple to implement, but with severe limitations. Image-space methods are a bit more involved and provide medium quality results. Object-space methods provide maximum quality and customizability, but often at the cost of speed. The miscellaneous category is a catch-all, but these methods tend to be quick and limited like hardware methods. The following sections survey significant methods in each category.

## 4. Hardware Methods

---

Hardware-based edge detection and rendering covers a wide variety of different methods. They all lack the need for mesh pre-processing, allowing them to be highly adaptable to new scenes and mesh animation. Edge detection is achieved as a by-product of their rendering modes and order, rather than a specific edge detecting step. They represent the first and simplest available methods of interactive edge detection.

Unfortunately, they are very limited in terms of customizability. They typically generate single pixel edges for which only the color can be changed. Unless combined with other techniques, they generally only detect contour edges.

### 4.1. Back-Facing Wireframe Contours

Jarek R. Rossignac and Maarten van Emmerik [Rossignac and Emmerik 92] described how to generate contour edges in their description of their Contour Edges with Hidden-lines Suppressed (CEHS) method. It only displayed a mesh's edges, not the mesh itself.

The part of the algorithm that deals with contour edges is:

1. Render the object's polygon into the z-buffer (nothing drawn to screen)
2. Shift depth buffer backwards
3. Increase the thickness of line rendering
4. Render the polygon in wireframe mode
5. Return the depth offset to its original position
6. Return line rendering to normal thickness

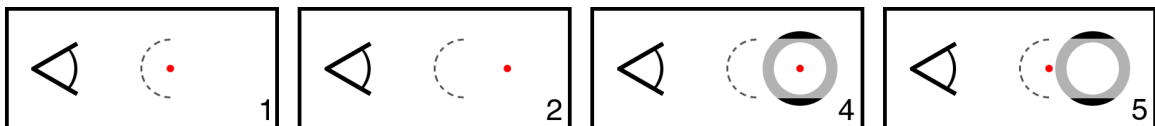


Figure 4-1: In step 1, the sphere mesh is rendered to the depth buffer (the dashed grey line) around the object origin (the red dot). In step 2, the origin is shifted back slightly. Step 4 renders the sphere's polygons in wireframe mode at the new origin using thick edges. The depth buffer's values prevent most of the edges from being rendered (grey areas). Step 5 shifts the origin back, preparing the scene for the next render.

By writing values to the depth buffer before shifting backwards, most edges are prevented from being drawn in step 4. Since the lines are rendered with additional thickness, lines on contour edges will poke out from behind the invisible "depth mask."

The color of these edges can be customized as desired. The thickness of the edge can also be controlled with the thickness value applied to the lines in step 3. Because line thickening does not round the ends of the lines it draws, sufficient thickness will result in gaps between adjacent edges. This can be alleviated by rendering a third pass where every vertex is rendered as a point, each thickened to the same degree as the edges.

Bruce and Amy Gooch [Gooch and Gooch 01] described a variation on Rossignac and van Emmerik's method.

The modified algorithm is:

1. Enable back-face culling
2. Set depth function to "Less Than"
3. Render the mesh in fill polygon mode (front-facing polygons only)
4. Enable front-face culling
5. Set depth function to "Less Than or Equal To"
6. Render the mesh in wireframe mode (back-facing polygons only)

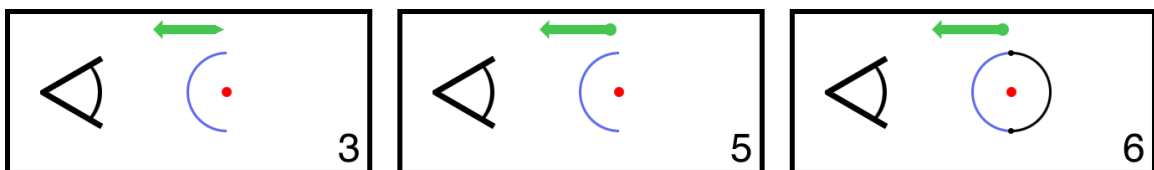


Figure 4-2: The green arrow represents the state of the depth function. In step 3, it is in less than mode. Steps 5 and 6 have the depth function in less than or equal to mode. The blue line represents the front-facing polygons and the black line represents the back-facing polygons in wireframe mode. The dots in step 6 represent points on the model where the depth function will overwrite front-facing pixels with back-facing pixels, creating the contour.

This variation favors changing how the depth buffer deals with values at the same depth, rather than offsetting the whole mesh. As a result, even though the back-facing pixels could be considered behind the previously rendered front-facing pixels, by default an edge with a maximum width of one pixel will still

render. Gooch and Gooch's modified method is faster than Rossignac and van Emmerik's method, because only half of the polygons are rendered in each pass.

One final variation combines the ideas of both above variations. Steps 2 and 5 of Bruce and Amy Gooch's method can be ignored if one desires contour edges that do not overlap the mesh at all. In this variation, the line thickness must be set greater than one to have any visible effect on the final image.

## **4.2. Back-Facing Filled Polygon Contours**

Ramesh Raskar and Michael Cohen [Raskar and Cohen 99] discussed several hardware-based methods of edge detection. Their first attempt was a step backward from the previously mentioned technique, but it was needed to reach their final, advanced technique.

The algorithm is virtually identical to Bruce and Amy Gooch's modifications above, except that wireframe rendering is replaced with filled polygon rendering. However, Raskar and Cohen's method was published first.

The algorithm is:

1. Enable back-face culling
2. Set depth function to "Less Than"
3. Render the mesh in fill polygon mode (front-facing polygons only)
4. Enable front-face culling
5. Set depth function to "Less Than or Equal To"
6. Render the mesh in fill polygon mode (back-facing polygons only)

Because the polygons are not scaled and cannot be thickened the way that lines can, rendered contour edges using this technique will be a maximum thickness of one pixel. Contour pixels may be missed or flicker due to z-buffer quantization and pixel sampling.

## **4.3. Offset Back-Facing Filled Polygon Contours**

Raskar and Cohen mentioned another technique that would allow for thicker edges. It uses depth offsets to force the back-facing polygons toward the

camera, pushing through the surface of the front-facing polygons at contour edges. More of the back-facing polygons' area will be rendered on top of the front-facing polygons than in previous methods.

The algorithm is:

1. Enable back-face culling
2. Set depth function to "Less Than"
3. Render the mesh in fill polygon mode (front-facing polygons only)
4. Enable front-face culling
5. Set depth function to "Less Than or Equal To"
6. Offset render depth towards camera a defined distance
7. Render the mesh in fill polygon mode (back-facing polygons only)
8. Return depth offset to normal

The thick edges this technique allows come at a dramatic cost. Since the back-faces are pulled through the front-faces, the orientation of the front-facing surface will determine the thickness of the edge. As a result, the overall thickness of the edge on the mesh will be uncontrollable and inconsistent for many meshes.

Unlike some previous methods, any thickness gained is at the expense of rendering the edge on top of the front-facing surface of the mesh. This effect may be desired, however.

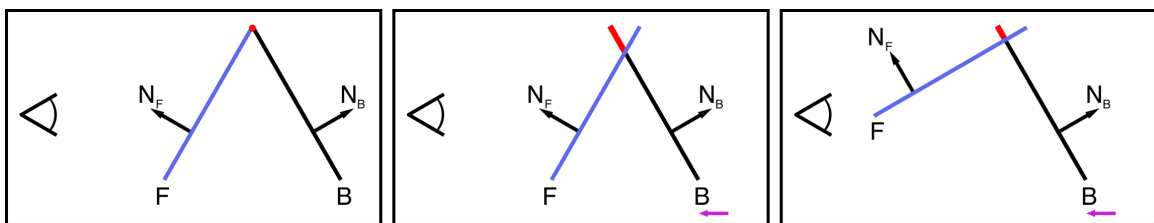


*Figure 4-3: The leftmost image shows the actual layout of the front (F) and back (B) facing polygons, and their respective normals. The red dot shows the location of the actual contour edge. In the second image, shifting the back-facing edges forward a distance equivalent to the purple arrow, they become the contour edge. However, the inconsistency with this method is demonstrated on the rightmost image: different front and back-facing polygon orientations will generate different thicknesses.*

#### 4.4. Thickness-Normalized Back-Facing Filled Polygon Contours

As one final step, Raskar and Cohen suggested another method to solve the inconsistent thickness problem while reducing the gapping problem of Rossignac and van Emmerik's wireframe thickening technique.

Assuming all mesh polygons are convex, the back-facing polygons' edges will be expanded outward a distance determined by their angle and distance from the camera. The result is that the actual edges are shifted out from behind the front-facing polygons the exact distance necessary to create a thickened border that is equally thick on all sides in screen-space. They call this process "polygon fattening."

Each edge should be shifted by:

$$(z * \sin(\alpha)) / \text{dot}(E, N)$$

In the direction:

$$\text{cross}(E, N)$$

Where  $z$  is the distance from the edge midpoint to the camera,  $\alpha$  is the angle between the edge vector and the view vector,  $V$  is the view vector,  $N$  is the polygon face normal, and  $E$  is the edge vector.

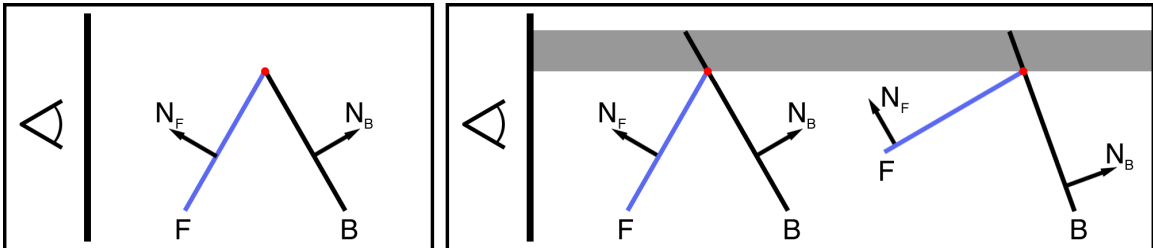


Figure 4-4: The shifted polygon edge maintains the same screen-space thickness despite the orientation of the polygons making up the edge.

However, this action of shifting the edges outward removes their connectivity. Without reconnecting them, they will not render as polygons. This is handled by creating new polygons that fit the shape of the outer edges as a triangle fan. This process causes the "capping" effect. Every back-facing polygon should be replaced with a set of  $2N$  polygons, where  $N$  is the number of edges in the

original polygon. The initial point to which all fan triangles connect should be the center point of the polygon.

The algorithm could be implemented:

1. Enable back-face culling
2. Render the mesh in fill polygon mode (front-facing polygons only)
3. Enable front-face culling
4. Loop through each back-facing polygon
  - a. Begin rendering triangle strip, using the polygon's center point as the initial point
  - b. Loop through each edge in order
    - i. Shift the edge outward
    - ii. Render both points to the triangle strip

It should be noted here that the gaps, while dealt with, are typically not completely filled as one might expect. How well the capping works is dependent on the desired thickness of the edge and the angle between each set of two connecting contour edges.

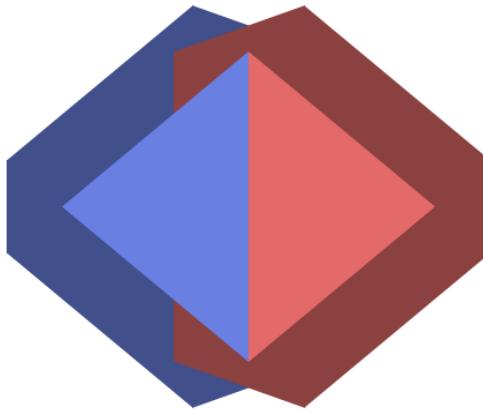


*Figure 4-5: Demonstrating edge fattening and its effects on capping. The brighter areas represent actual polygons from which the darker areas are calculated. Along contour lines, the fattened back-facing polygons will partially stick out from behind the front-facing polygons.*

#### **4.5. Stencil-Based Pixel Shifted Silhouettes**

Tom McReynolds and David Blythe [McReynolds and Blythe 99] described a method that renders the object multiple times to the stencil buffer, each time at a

slight offset on the x and y axes. By rendering an edge-colored quad over the object with certain stencil pass rules, the silhouette edges of the previously rendered object will appear.

The algorithm is:

1. Render the shaded mesh, if desired
2. Clear stencil buffer to zero
3. Disable color and depth buffers
4. Set stencil buffer to always pass, the operation to always increment
5. Shift the viewport by one in the positive y direction
6. Render mesh
7. Shift the viewport by two in the negative y direction
8. Render mesh
9. Shift the viewport by one in the positive x direction and one in the positive y direction
10. Render mesh
11. Shift the viewport by two in the negative x direction
12. Render mesh
13. Shift the viewport by one in the positive x direction (original position)
14. Enable color and depth buffers
15. Set stencil buffer to pass at two or three (the second bit equal to 1)
16. Render edge-colored quad that covers the mesh

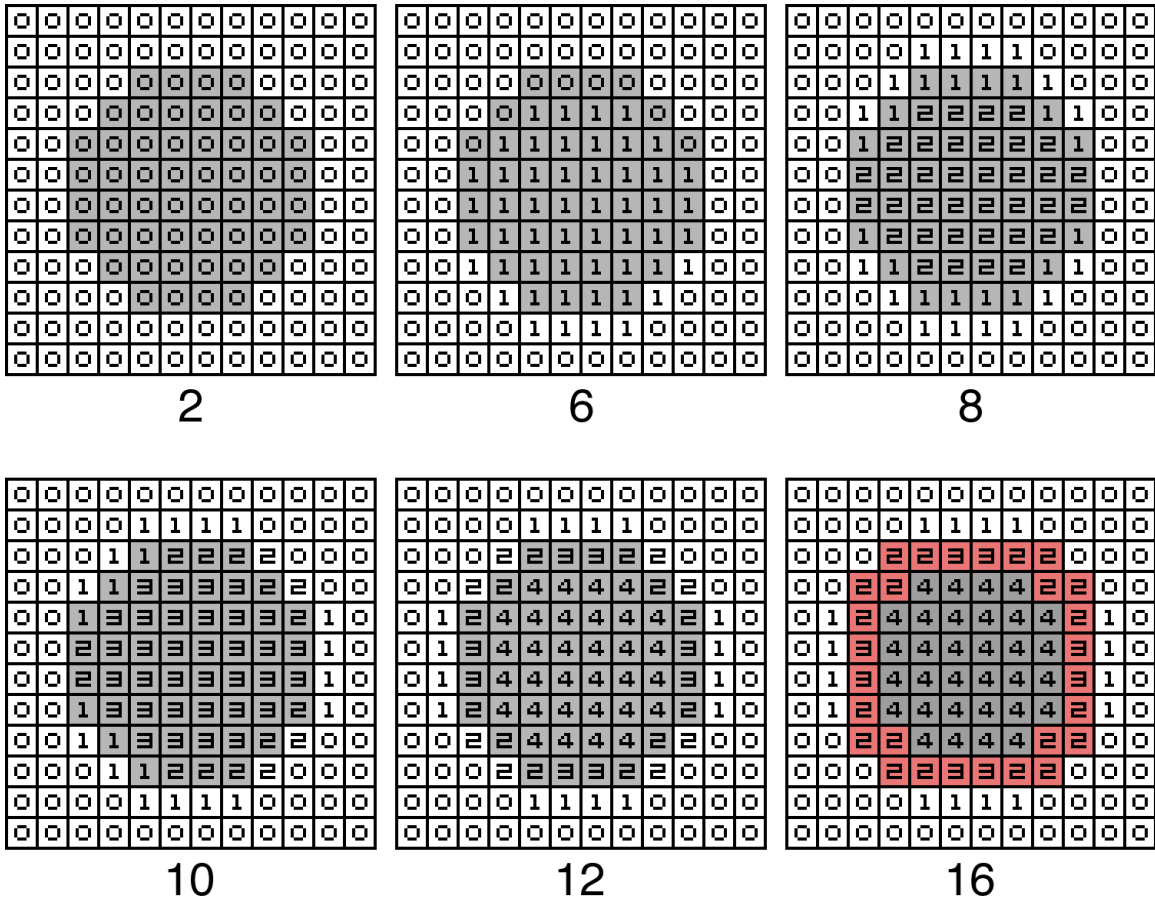


Figure 4-6: The above illustrations show the state of the stencil buffer after each corresponding step. The grey area represents the actual drawable mesh pixels. In the last frame (16), the red indicates which pixels would form the edge.

This method is relatively slow because the scene must be rendered at least four times per frame.

#### 4.6. Inverted Stencil Contours

A faster, less accurate method of stencil-based edges by K. Akeley was mentioned in McReynolds and Blythe's class. It only requires one render to the stencil buffer and uses wireframes rather than filled polygons.

The algorithm is:

1. Clear stencil buffer to 0
2. Set stencil function to always pass and the operation to invert
3. Enable back-face culling
4. Render mesh in wireframe mode (front-facing polygons only)

5. Set stencil function to pass if the value is 1
6. Render edge-colored quad that covers the mesh

This works because wireframe edges that are part of two adjacent polygons will be drawn twice, inverting their stencil pixels back to zero. However, the pixels on the polygon edges between front and back-facing polygons will only be drawn once, and will have a stencil buffer value of 1.

This technique will also generate front-facing boundary edges, but not back-facing boundary edges. McReynolds and Blythe suggested that the technique be combined with the drawing of all visible boundary edges to complete the edges. They blocked the inclusion of invisible boundary edges by first rendering an offset depth buffer that would prevent covered edges from rendering. This method is also susceptible to stencil rendering interference if the whole scene is processed for edges at once.

#### **4.7. Hardware Creases and Contours**

Ramesh Raskar [Raskar 01] released a paper describing a hardware method to render crease edges in addition to contours. Though the technique takes advantage of the geometry shader and a secondary depth-buffer, it does not use a specific edge-detecting step.

The contours are rendered by expanding all back-facing polygons a user-defined distance, based on the screen-space projection width, similar to Raskar's previous method. After shifting all of these polygon's edges outward, the expanded edges are then reconnected into solid polygons and rendered black to create the contours.

For creases, the ridge and valley varieties are created differently. The ridge creases are created by generating a new quad with a length and location equivalent to each front-facing polygon edge in the geometry shader. When it is first created, this new quad should be flush with the polygon surface. Before sending it to the remainder of the pipeline, it should be rotated the user-defined

dihedral angle about the edge vector, and thickened the same way as the contour edges so that all edges have a consistent thickness.

Since the quad is rotated the dihedral angular distance from the originating polygon, these edges will only appear if the adjacent polygon connects with an angle sharper than the one defined by the user, creating the crease edge. This can create z-fighting if the user's dihedral angle is equivalent to the angular distance of two connected polygons.

Valley creases are far more complicated to create. They, like the ridge creases, use a user-defined dihedral angle to determine where to create expanded polygon edges as quads. However, the visibility requirements for valley edges are the reverse of those needed for the ridge creases. To solve this, Raskar created a dual depth buffer. With two depth buffers, the created valley crease quad will only be allowed to modify the final image if it renders in-between the two depth values.

Finally, Raskar's method defined a way to detect self-intersection edges using the dual depth buffer technique again.

## 5. Image-Space Methods

---

Image-space edge detection and rendering utilizes image processing techniques to detect discontinuities in one or more rendered images. This operation may have variations in what image(s) is used as input, what type of image processing is used, and how the output information is utilized.

### 5.1. Image Processing with the Sobel Operator

For edge detection, image processing techniques typically apply convolutions to various properties of images or specialized images to generate gradients, a vector representing the local maximum change. In image processing, convolutions take the form of component-wise matrices called kernels or operators. These operators store numbers in each cell which are multiplied by some numerical property of the equivalent pixel in the input image. This operation is applied to every pixel in the input image, with optional special cases at the image borders where input data may not be available. The resulting output image data can be used in further calculations or displayed directly.

For each pixel ( $x$ ) there are surrounding pixels (A, B, C, D, E, F, G, and H) except at the extreme borders of the viewport. The layout is:

$$\begin{bmatrix} A & B & C \\ D & x & E \\ F & G & H \end{bmatrix} = L$$

L represents the input pixels that will be used in conjunction with a kernel. Since a pixel is typically made up of color and alpha transparency information, the user must decide what property of the input image pixels he will use. The two most common types of information used will be described later.

The Sobel operator [HIPR 00] will be used to illustrate how operators are applied to input images. The Sobel operator detects gradients in the horizontal and vertical axes separately.

The typical Sobel operators are:

$$\begin{bmatrix} -1 & 0 & 1 \\ -2 & 0 & 2 \\ -1 & 0 & 1 \end{bmatrix} = G_x \qquad \begin{bmatrix} 1 & 2 & 1 \\ 0 & 0 & 0 \\ -1 & -2 & -1 \end{bmatrix} = G_y$$

When one applies the Sobel operator to a given pixel, a component-wise multiplication is applied and then the inner terms are summed:

$$LG_x = (-A) + C + (-2D) + (2E) + (-F) + H;$$

$$LG_y = A + (2B) + C + (-F) + (-2G) + (-H);$$

The  $LG_x$  and  $LG_y$  terms can be used to determine the direction of the gradient, but for the purposes of edge detection, only the magnitude of the gradient is needed.

The gradient magnitude is calculated:

$$|G| = \sqrt{LG_x^2 + LG_y^2}$$

However, for most purposes, the gradient magnitude can be approximated by:

$$|G| = |G_x| + |G_y|$$

The gradient magnitude can be used directly in edge detection. By drawing black pixels where the gradient magnitude is greater than or less than a user-defined value, edges will be rendered. The process of choosing which pixels to draw based on the gradient (or any value) is called thresholding.

## 5.2. Other Operators

The kernel most often used by real-time graphics applications is the Sobel operator. However, in image processing literature, there are several other edge-detecting operators. Below is a list of other operators from Wikipedia and Hypermedia Image Processing Reference [HIPR 00] that might be used.

### ***Prewitt Operator***

$$\begin{bmatrix} -1 & 0 & 1 \\ -1 & 0 & 1 \\ -1 & 0 & 1 \end{bmatrix} = G_x$$

$$\begin{bmatrix} -1 & -1 & -1 \\ 0 & 0 & 0 \\ 1 & 1 & 1 \end{bmatrix} = G_y$$

### ***Scharr Operator***

$$\begin{bmatrix} 3 & 0 & -3 \\ 10 & 0 & -10 \\ 3 & 0 & -3 \end{bmatrix} = G_x$$

$$\begin{bmatrix} 3 & 10 & 3 \\ 0 & 0 & 0 \\ -3 & -10 & -3 \end{bmatrix} = G_y$$

### ***Robert's Cross Operator***

Robert's Cross Operator works with a smaller data set and is therefore less accurate. The unusual size of the kernel means that the "central" pixel is on the upper left-hand side. Otherwise, it operates under the same principle as the other operators.

$$\begin{bmatrix} x & A \\ B & C \end{bmatrix} = L$$

$$\begin{bmatrix} 1 & 0 \\ 0 & -1 \end{bmatrix} = G_x$$

$$\begin{bmatrix} 0 & 1 \\ -1 & 0 \end{bmatrix} = G_y$$

### ***Operator Variations***

There are several other versions of the Sobel operator with different numbers, dimensions, and calculation schemes. These variations are meant to gain various accuracy or detection abilities not available with the version of the Sobel

operator described above [Kroon 09]. Variations exist for the other operators as well. These variations are beyond the scope of this thesis.

### **5.3. Input Imagery**

In traditional image processing, the input image is typically a grayscale version of the image for which edges are desired. A grayscale image provides a single value from zero to one that represents the intensity at each pixel. Dealing with image noise and non-edge areas of high gradient magnitude are very difficult to overcome with only the original image available. Real-time graphics provide more flexibility. While the scene could be rendered in grayscale form and then used for edge detection on a second pass, edges can be detected with more accuracy using visualizations of scene information.

#### ***Depth Buffer Usage***

Takafumi Saito and Tokiichiro Takahashi [Saito and Takahashi 90] used the scene depth information as their input image. On the first pass, the scene's depth information is rendered and retrieved. Variations of the Sobel operator are used to obtain first and second-order differential data. After thresholding and other error adjustment, the resulting information is rendered to create an edge image. They also explored methods of using the edge information to enhance the fully shaded image beyond merely overlaying the edges.

The difficulty with using only the depth information for the edge test is that while depth buffers can be used to detect contour edges, they are not very good for use in detecting crease and intersection edges, as surrounding pixels have very similar depth information. Additionally, depth buffer resolution limitations can prevent the adequate detection of edges on objects at similar depths.

#### ***Normal Buffer Usage***

Philippe Decaudin [Decaudin 96] suggested using the scene's normal information to supplement the depth buffer information. Normals rendered as colors very distinctly show crease and intersection edge discontinuities. Most edges can be found using both gradient magnitudes together.

Since a normal is a 3D vector, the user may choose to do the edge detection on all three dimensions of the normal and then sum the resulting modified values. Otherwise, a one dimensional component of the normal buffer at each pixel is required. One simple possibility is the dot product of the view and normal vector. Another is the grayscale version of the normal buffer, which can be found by summing of the normal's axes and then normalizing the result. As with the depth buffer, the resulting gradient image must be thresholded to get only the desired edges.

#### **5.4. Modern Implementation**

When Saito & Takahashi and Decaudin wrote their respective papers the graphics hardware available required them to transmit the rendered images back to the CPU each frame. While the depth information could be retrieved directly, the normal color information had to be created by rendering the scene twice with special lighting conditions before the image was transmitted back to the CPU for image processing. Once the image was processed, it had to be sent back to the graphics card where the edge information and other shading were combined to create the final image.

Modern graphics cards provide programmable shaders and framebuffer objects. The shaders allow for the more specific and easier creation of depth and normal imagery. The framebuffer objects allow the graphics card to create offscreen renders that can be held over into subsequent frames without interfering with imagery rendered to the screen. With these two improvements, image-space edge detection can be accomplished with two rendering passes without any significant data transfer to or from the graphics card. [Card and Mitchell 02]

In the first pass, all the scene's geometry should be rendered with a special shader that does not send its data to the screen. Instead, the fragment (pixel) shader calculates normal information at each pixel from the vertex normals. The 3D normal information is stored in the RGB components of a framebuffer object created prior. The depth information, whether calculated manually or not can be stored in the alpha channel of the same framebuffer object that contains the

normal information. Optionally, additional framebuffer objects can be created to hold other information such as the shade color at each pixel.

In the second pass, a screen-aligned quad with UV coordinates that prevent wrapping is rendered instead of the scene. In the shader, the UV coordinates of the quad are used as lookups into the framebuffer object rendered in the previous frame. At this point, the edge detection methods are performed at each pixel for both the normal and depth information. Generally, the sum of the edges found in both sets of information are used together to represent all edges, though there is plenty of room for customization. Finally, the edge information is combined with any other shading information rendered in the previous pass to create the final output color for each pixel. The output of these operations will be an edge or edge-enhanced image.

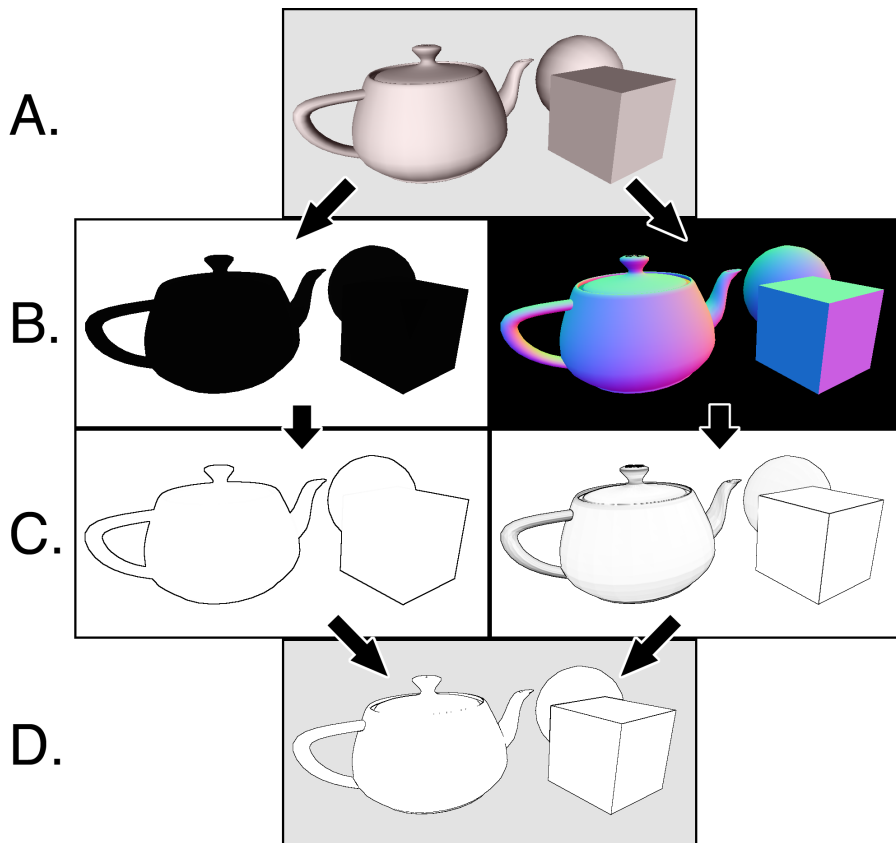


*Figure 5-1: A shaded scene (A) may be rendered using the image-space edge detection by doing a pass where depth (left B) and normal (right B) information are rendered to framebuffers. In the next pass, while rendering a screen-sized quad, the two framebuffers are used by an image processing operator to get their respective gradient magnitudes (C). The gradient magnitudes are thresholded and combined to create the final output (D).*

## 5.5. Technique Variations

Image-space edge detection is often the method of choice when detecting edges for the purpose of anti-aliasing because they overlap both sides of the edges detected. For this use, areas determined to be edges are used as a mask for a blur operation. This creates an inexpensive anti-aliasing effect that is especially well-suited to deferred shading.

Additional scene information could be used to further augment the edge detection. For example, providing every object a unique color would allow silhouette edges to be detected even of the objects shared nearly identical depths and surface normals in the edge areas. Unique colors could also be given to distinct object faces to prevent missed edge cases where an object is folded over itself, as described in Aaron Hertzmann's paper [Hertzmann 99].

## 5.6. Advantages and Disadvantages

Image-space edge detection has two distinct advantages over other edge detection techniques:

- Constant edge detection speed
- Natively detects intersection edges

Because the number of edge detecting operations is directly dependent on the screen size, rather than the number of objects, the edge detecting step of the second pass will perform at the same speed no matter how simple or complex the scene is. The first pass is still limited by the hardware and how complicated the scene is, however.

Intersection edges are discontinuities that don't correspond to polygon edges. However, in image-space, intersection edges are merely another variation of a surface discontinuity.

The disadvantages are:

- Lack of customizability
- Missed edges

- False positive edges
- Relatively high tweaking required to get accurate results

The thickness of the edges can't be directly controlled. The only way to get thicker edges is to apply further image processing or do the edge detection of buffers that are larger than the output resolution. Though these edges may be colored, only screen-space texturing is possible.

Depending on the threshold settings, legitimate edges can be missed entirely. The thresholding might also create false positive edges, where the rate of change, while smooth, was too great to be ignored by the image processing.

The thresholding values must be tweaked by the user to achieve the desired results. These threshold values are sensitive to the object, the rendering purpose, and the user's own preferences. More trial and error is required for image-space edge detection than for other techniques.

## 6. Object-Space Methods

---

The object-space method of edge detection seeks to identify drawable edges in three dimensional space. At its most basic, all unique polygon edges are checked for drawability given a camera position and other factors. All variations on the basic idea are implementation details, supplemental features, and attempts to significantly reduce the number of tests necessary.

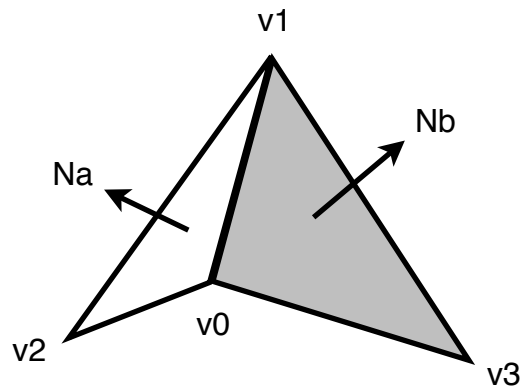


*Figure 6-1: A single polygon edge connecting two adjacent polygons. Na and Nb are the face normals for the two adjacent polygons. v0 and v1 vertices define the edge. v2 and v3 complete the two adjacent polygon's vertices. The right polygon, and therefore the v3 vertex, may not exist. If so, the edge is a boundary edge.*

### 6.1. Drawable Edge Tests

The definition of each edge type defines a simple formula for determining if a polygon edge is drawable from a given perspective. Refer to figure 6-1 for a graphical reference of the terms used below.

#### **Contour Edge**

$$(\text{dot}(\text{Na}, V) * \text{dot}(\text{Nb}, V)) < 0$$

Where Na and Nb represent the face normals for the two polygons adjacent to the polygon edge and V represents the view vector, pointing from one of the edge vertices toward the camera. All vectors should be normalized. [Marshall 01]

Na and Nb can be calculated:

$$\text{Na} = \text{normalize}(\text{cross}((\text{v1} - \text{v0}), (\text{v2} - \text{v0})));$$

$$\text{Nb} = \text{normalize}(\text{cross}((\text{v3} - \text{v0}), (\text{v1} - \text{v0})));$$

V can be calculated:

```
V = normalize(CameraPosition - v0);
```

The dot product of two normalized vectors is the cosine of the angle between them. For vectors greater than 90 degrees apart, the result of a dot product is negative. Two back-facing or two front-facing polygons will result in the multiplication being positive. Therefore, by multiplying the dot product results together, only cases where one polygon or the other is back-facing, but not both, will render the contour test true.

### **Crease Edge**

```
dot(Na, Nb) < -cos(θ)
```

Where  $\theta$  is the user-defined dihedral angle. All vectors should be normalized.

The dihedral angle measures the angle between two planes, which are the two adjacent polygons in this case. However, the dot product is the cosine of the angle between the face normals. The dihedral angle and the angle between the normals form an inverse relationship, hence the negating of the cosine operation on the right. The crease test will render true if the angle between the polygons is smaller than the dihedral angle.

To differentiate between ridge and valley crease edges, the following modifications can be made to the test [McGuire and Hughes 04]:

### **Ridge Crease Edge**

```
(dot(Na, Nb) < -cos(θr)) && (dot((v3 - v2), Na) <= 0)
```

### **Valley Crease Edge**

```
(dot(Na, Nb) < -cos(θv)) && (dot((v3 - v2), Na) > 0)
```

Where  $\theta_r$  and  $\theta_v$  are the ridge and valley dihedral angles, respectively. All vectors should be normalized.

The right side of the test differentiates ridges and valleys by comparing the vector pointing from  $v_2$  to  $v_3$  to the face normal  $N_a$ . This is because the  $N_a$  points away from  $v_3$  when the edge is a ridge, and it points towards  $v_3$  when the edge is a valley.

The differentiation of crease edges into ridge and valley varieties was included for completeness and will not be mentioned further.

### ***Boundary Edge***

Since boundary edges are based on the structure of the mesh and do not cease to be boundaries when the mesh animates, these edges should always be pre-calculated and flagged as drawable.

### ***Marked Edge***

Similar to the boundary edge, these edges are always pre-calculated. They should be flagged as drawable.

### ***Intersection Edge***

These do not correspond to polygon edges, so they are not handled by object-space methods. They will not be discussed further in this section.

## **6.2. Edge Detection**

The most basic object-space method requires that the mesh be preprocessed into an edge mesh, which stores adjacency data for the mesh's polygon edges. It should contain the two edge vertices and the one or two other vertices that define the one or two triangles attached to the edge. Every polygon edge should get one and only one entry, unless modifications or optimizations require more.

How this is implemented is determined by the needs of the architecture. If possible, it is beneficial to store the edge mesh in terms of indices into the vertex array, rather than making duplicates of the vertices. Doing so will significantly reduce the amount of memory needed to store the edge mesh.

Detecting the edges simply involves looping through each entry in the edge mesh to determine if it fits the criteria for being drawable. Boundary, marked, and pre-calculated crease edges can be flagged as always drawable by setting the v3 entry equal to the v0 entry. One could also specifically differentiate the various pre-calculated drawable edges by setting v3 equal to v1, or v2 equal to v0 or v1. This edge mesh setup closely resembles McGuire's [McGuire and Hughes 04]. Others exist and a few of them are mentioned below.

### ***Optimizations and Variations***

Markosian et al. [Markosian et al. 97] used complete adjacency information, storing references to all connecting vertices at each end of the edge. By doing so, drawable edges could be traversed along their entire length. This traversal ability removed the need to test every edge every frame. They randomly checked a portion of the edges for drawability.

When a drawable edge was found, adjacent edges were also checked for drawability until no more drawable edges could be found. Doing this allowed them to detect the longest, and therefore the most relevant, edges with a minimum number of random tests. Because edges tend to stay the same from frame to frame, a portion of drawable edges from the previous frame were tested first.

Markosian et al. found a fivefold increase in speed using these optimizations over testing all edges. Of course, edges can be missed entirely from frame to frame, so some accuracy is lost. They also used and improved some hidden edge removal algorithms which prevented occluded edges from being drawn.

Gooch et al. [Gooch et al. 99] described a method where they stored edges' normal arc on a sphere surrounding the object. Groups of similar arcs, in gauss map format, were stored hierarchically so that groups of edges could quickly be deemed all back-facing or all front-facing. A plane was placed at the origin of the sphere and then aligned perpendicular with the view vector. Edges whose arc intersect the plane are contour edges. This technique allowed contour edge detection to be sped up by 1.3 times for their S. Crank mesh and 5.1 times for a sphere. Unfortunately, this technique only works well under orthographic projection.

In a similar idea, Sander et al. [Sander et al. 00] created a hierarchical search tree of polygons. At each node, they created anchored cones that represented the maximum range of the normals possessed by vertices in the node. This information can be used to quickly determine that no contour edges are possible for whole sets of nodes without testing individual edges.

John W. Buchanan and Mario C. Sousa [Buchanan and Sousa 00] defined a different kind of edge mesh that helped in the testing for contour, boundary, and marked edges. It combined the edge detection into the polygon rendering, significantly reducing the impact of edge detection on rendering time. However, it assumed the processing of individual polygons during the rendering process, which is no longer common thanks to vertex buffer arrays.

Jeff Lander [Lander 01] documented the optimization of ignoring edges that have co-planar adjacent polygons. Flat planes only generate drawable contour edges on their outside edges, not their internal edges, and they lack the angular difference between adjacent polygons to generate crease edges. During the preprocessing step, an additional test checks for co-planar adjacent polygons. If found, the edge is not added to the edge mesh.

Depending on how the mesh is created and how many flat areas it has, the savings in the number of needed edges can be significant. For example, the author found that 22.3% of the edges in the Utah Teapot can be safely ignored, and an amazing 50% of a cylinder's edges can be ignored. Low-polygon meshes, typically created using triangles instead of quads have a much lower number of ignorable edges. Only 1.6% of Blender's Suzanne Monkey model can be ignored.

Morgan McGuire and John F. Hughes [McGuire and Hughes 04] detailed a method to shift the entirety of the edge detection and rendering to the graphics card via programmable shaders. Copies of adjacency, vertex, and normal information were stored in vertex buffer arrays and accessed within the vertex shader. If the edge was found renderable, the degenerate duplicate vertices were turned into screen-aligned quads. Otherwise, they were shifted behind the camera, where they would be clipped during the rendering process. McGuire and Hughes also took a critical look at how the thick edge gaps could be filled effectively. Since McGuire and Hughes' paper had a major influence on this thesis, its algorithms and features will be more specifically described later.

Still other variations exist. Aaron Hertzmann and Dennis Zorin [Hertzmann and Zorin 00] described a method of using 4D dual surfaces to determine the contour edges with curve-plane intersections. Tom Hall [Hall 03] created a modification of Markosian et al.'s technique by focusing almost exclusively on tracking contour changes from frame to frame. By looking at adjacent edges to previously found edges and noticing the relative camera change, he was able to significantly reduce the number of edges tested. His method worked especially well with highly tessellated meshes.

### **6.3. Edge Rendering**

In object-space edge detection, the rendering is a distinctly different process from the detection. After a polygon edge has been determined drawable, the user has the choice of what to do with that information. The possible edge effect is highly dependent on the technology available and speed requirements. In this section, several methods of edge rendering are discussed.

#### ***Line Edge***

The simplest method of drawing the edges is to create a rasterized line between the two edge points:  $v_0$  and  $v_1$ . If the hardware supports it, thick edges can be created by specifying these rasterized lines be greater than one pixel in width. This method is very fast and requires no additional processing of the edges. One advantage rasterized lines have over a single pixel-width quad is that no matter their orientation, they always render a single pixel on the edge. A single pixel-width quad can get rendered to less than a single pixel at some orientations, creating artifacts. However, these lines can only be customized in terms of their color. They cannot be textured.

#### ***Quad Edge***

By expanding edges into screen-space quads, they can be made as thick as the user desires, textured, and/or anti-aliased. McGuire and Hughes [McGuire and Hughes 04] worked almost exclusively with this method. They constructed two types of edges from quads: full and half quad edges.

Full quad edges were made by generating the screen-space perpendicular vector, scaling it, and using it to offset the points of the edge on both sides. This generated a thick quad around every drawable edge.

Half quad edges were used mainly for contours. Since each edge is on the surface of the mesh, contour edges would have half of their quad rendered below the surface. This can lead to artifacts. Half quad edges only render on the “outside” of the mesh, pointing in the same direction as  $v_0$ 's vertex normal  $n_0$ , solving the artifact problem.

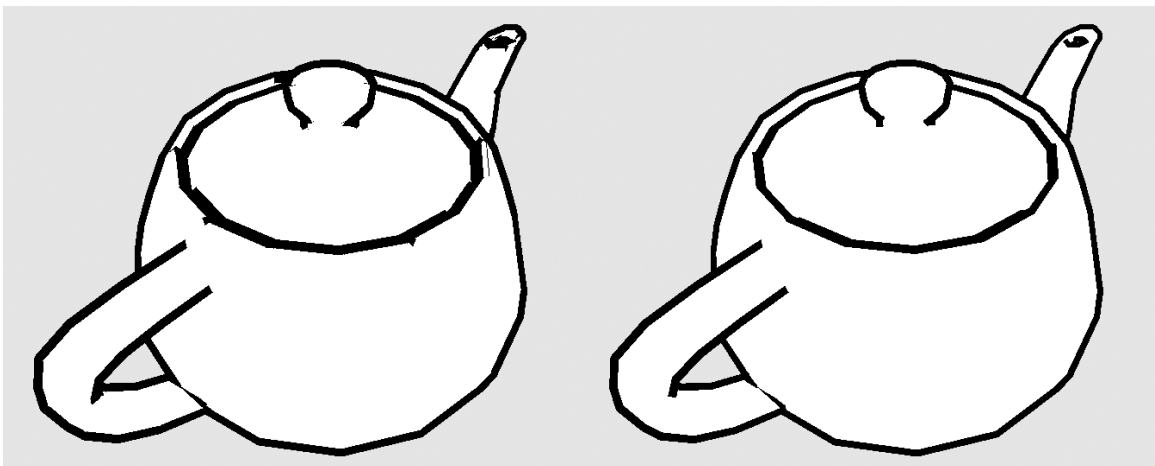


*Figure 6-2: The full quad method (left) has artifacts on the spout and lid where the bottom half of an edge pushes through the surface. Using half quad edges for the contours (right), these artifacts are eliminated.*

Like any quad, these edges can be textured, anti-aliased, or shaded as the user desires. Adjusting the scaling factor for the perpendicular vector allows thickness control.

### ***Other Artistic Edges***

J.D. Northrup and Lee Markosian [Northrup and Markosian 00] connected related edges together to form a few sets of long, connected edges. They then expanded the edges into connected screen-space quads, which were easily textured. Using this connection step, textured strokes could easily extend beyond the bounds of a single polygon edge's screen-space length. Such realistic stroke parameterization is difficult when edges are treated independently.

Jeff Lander [Lander 01] used multiple rasterized lines rendered at slight distance and rotational offsets to get a sketchy look. Marc ten Bosch [Bosch 06] created a method of partial edge detection that faded edges in as they approached visibility, and faded them out as they approached invisibility. This reduces the sometimes problematic popping effect that occurs when the contour edge from the previous frame shifts to another polygon edge.

#### 6.4. Thick Edge Gaps

When rendering thick edges as thick lines or screen-space quads, non-parallel connecting edges will have visible gaps. These gaps get worse as the edges are made thicker. There have been a few attempts to address this problem.

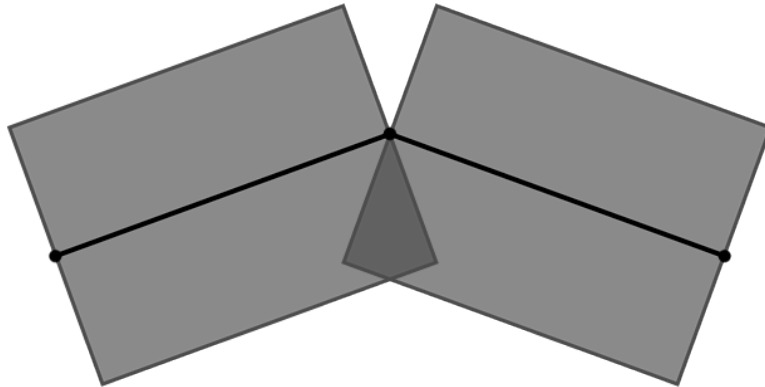


*Figure 6-3: Two connected drawable edges. Since they are not parallel, they create a gap above their connection point.*

Bruce Gooch et al. [Gooch et al. 99] suggested that a single, thick point be rendered at both ends of any drawable edge. While this will smoothly solve the gap problem, thick rasterized points are not always available. Additionally, these points can generate the same artifacts as full quad edges on contours, and they interrupt edge texturing.

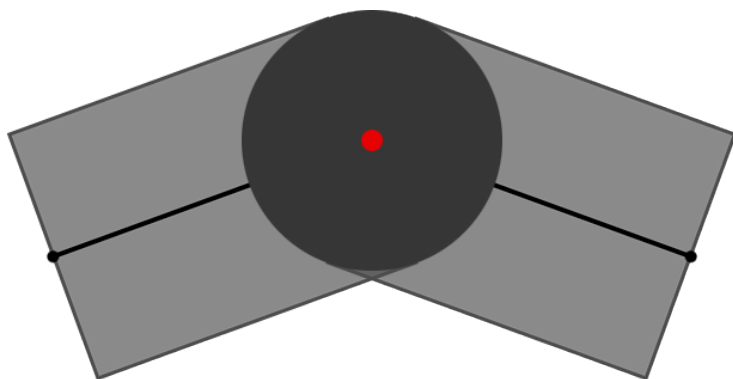


Figure 6-4: The red dot represents the screen-space vertex where the two edges connect. A single dark grey point is drawn there with a thickness equivalent to the edges' thickness.

Morgan McGuire and John F. Hughes [McGuire and Hughes 04] solved the gap problem with the limited resources of the GPU shader environment by rendering two extra cap-passes, where they generated triangle caps on both ends of the edge. The caps of connecting edges' triangle caps shared a vertex along the vertex normal projected into screen-space, which allowed the caps to line up in most cases. They also found a way to implement texture parameterization on these caps such that they wouldn't interfere with the texturing of the edges they connected to. There were a few problematic cases, however, when the vertex normals' screen-space projections did not reflect the curvature of the edge, resulting in caps on the wrong side. They suggested generating caps on both sides of the edge in cases where such failure was likely. To make smoother caps, they also suggested that caps could be generated out of a triangle fan, rather than a single triangle, but at the expense of many additional render passes.

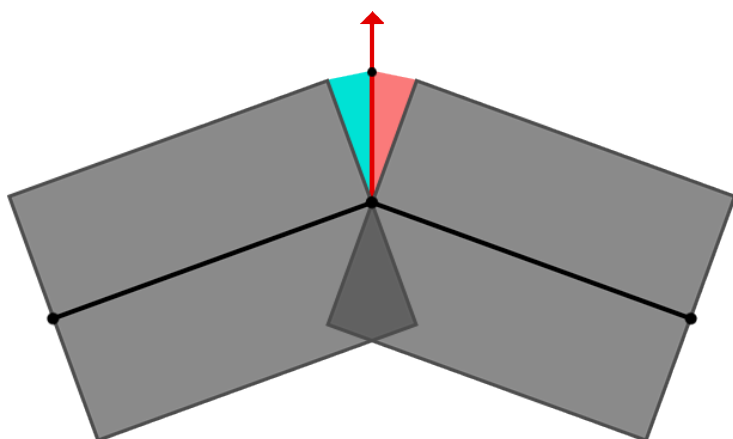


Figure 6-5: Using the red screen-space normal, both the left and right edges will generate half of the cap that fills the gap.

## 7. Miscellaneous Methods

---

This category is a catch-all for those methods that don't fit well in other categories. Thus, there are no real similarities among the methods listed.

### 7.1 Surface Angle Contours

Surface angle contours take advantage of the fact that as the surface of a smooth mesh approaches a contour, the normal becomes closer and closer to perpendicular to the view vector. The contour occurs on the surface at exactly the points on the surface where the view and normal vector are perpendicular.

Theoretically, the surface could be shaded black when the normal is exactly perpendicular to the view vector. However, meshes are made of flat polygons and their edges can be completely missed if using only the exact perpendicular pixels. Thus, the surface angle contour method always uses a range of values close to the perpendicular to indicate edges, regardless of implementation.

Gooch et al. [Gooch et al. 99] briefly mentioned the use of an environment map containing black color on the outer rim, forming a dark circle. Since the outer rim of the environmental map is where the calculated reflection direction of the near-perpendicular surface areas will access, the surface near the contours get rendered black.

Carl Marshall [Marshall 01] implemented the idea using a pixel shader. At each surface pixel, the dot product of the view and normal vector was used to index into a 1D texture that contained a dark color at the lower end. Additionally, one could simply threshold the dot product value to render black below a certain value, as displayed in Figure 7-1.

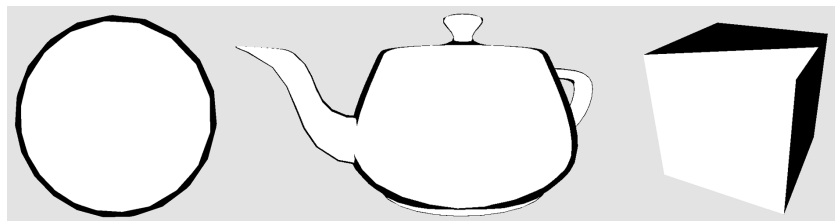


*Figure 7-1: This variation uses a thresholding dot product check in a pixel shader. Some objects work better than others with this method, but the edge width is almost always inconsistent. The cube illustrates the main failure case for this method.*

Though this method is extremely simple and inexpensive, it yields inconsistent results for some meshes. This method fails to correctly handle flat surfaces.

## 7.2 Expanded Inverted Geometry Contours

Christopher Evans [Evans 03] described this method in a tutorial. The technique creates contour edges by rendering the mesh twice. The first pass renders the object normally, with whatever shading desired. The second pass, however, renders the same object scaled up slightly, with no shading, colored black, with its normals inverted, and back-face culling enabled. The combination of back-face culling and inverted normals only allows the back side of the scaled object to render, forming outlines for the object.

This method is extremely simple to implement and has a different visual effect than similar hardware methods. However, it also shares the multiple renders and relative lack of customizability of hardware methods.



*Figure7-2: The black edges are actually a scaled version of the bomb, rendered with back-face culling, inverted normals, and no shading. Some artifacts are generated, but it generally gives pleasing results. (Image courtesy of ChrisEvans3D.com [Evans 03])*

## 8. Morgan McGuire and John F. Hughes' Hardware-Determined Feature Edges

---

The author focused heavily on improving the object-space method described by Morgan McGuire and John F. Hughes [McGuire and Hughes 04]. To provide context and ease understanding, the author here details McGuire and Hughes' work as it relates to the author's contributions.

McGuire and Hughes' goal was to transfer all detection and rendering of edges to the graphics card, gaining the speed of parallel calculation and removing the bottleneck of geometry data transfer from the CPU to the GPU. Parallel computation and the technology of the time forced them to test every polygon edge independently, unlike some of the object-space optimizations. As a result, a large amount of GPU memory is required.

The method used four render passes:

- Mesh pass - Render mesh normally at a slight backward offset
- Edge pass - Render drawable edges as expanded quads or lines
- Cap pass (first side) - Render the first side cap of each drawable edge
- Cap pass (second side) - Render the second side cap of each drawable edge

### 8.1. Data Structure

McGuire and Hughes created an edge mesh data structure that contained four edge vertices for each unique polygon edge. Each edge vertex contained values required for edge detection and generation. Those that can be represented geometrically are shown in Figure 8-1.

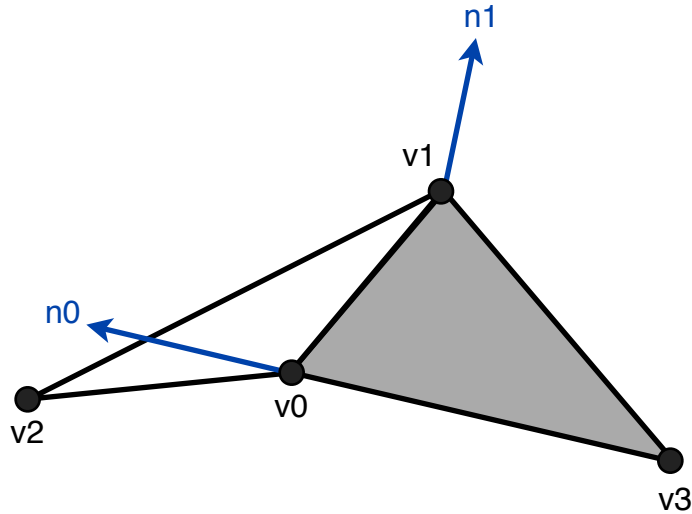


Figure 8-1: The important geometric values for each edge in McGuire and Hughes' method:  $v_0$ ,  $v_1$ ,  $v_2$ , and  $v_3$  are vertices on two polygons that share an edge.  $n_0$  and  $n_1$  are the vertex normals for  $v_0$  and  $v_1$ , respectively.

The values in each edge vertex are:

- $v_0$  - first vertex in the edge
- $v_1$  - second vertex in the edge
- $v_2$  - final vertex that, with  $v_0$  and  $v_1$ , makes the first polygon
- $v_3$  - final vertex that, with  $v_0$  and  $v_1$ , makes the second polygon
- $n_0$  -  $v_0$ 's normal vector
- $n_1$  -  $v_1$ 's normal vector
- $r$  - random scalar used in texture parameterization
- $i$  - scalar from 0 to 3 that differentiates duplicates in the edge mesh

$v_0$ ,  $v_1$ ,  $v_2$ ,  $v_3$ ,  $n_0$ , and  $n_1$  are all 3D vectors.  $r$  is used only for object-space texture parameterization.  $i$  is used to pick different output vertices in the vertex shader so that the edge will become non-degenerate. If the edge is a boundary edge, there is no  $v_3$  vertex. In that case,  $v_3$  should be set equal to  $v_0$ .

For each polygon edge, all of the above values are obtained from the mesh, except for  $i$ . The newly formed edge vertex is duplicated three times. Each of the now four edge vertices with the same data are given a different, ordered  $i$  value from 0 to 3. All four of these edge vertices for each polygon edge is stored with all other edge vertices in an edge mesh. Finally, the edge mesh is copied into

vertex buffers on the GPU for later use. This preprocessing step is quite expensive, but once complete, all edge detection and rendering can be accomplished by the GPU with no special data transfer whatsoever.

The user needs some way of referencing the edge mesh buffers on the GPU. Generating an index array buffer containing sequential numbers from 0 to  $(4E - 1)$ , where  $E$  is the number of unique polygon edges, allows the data to be referenced and rendered with a single render call. Furthermore, other index array buffers can be created to reference only the first three, or first two,  $i$  values of each set of four edge vertices. Such index array buffers are useful for rendering caps and thin edges.

## 8.2. Edge Detection

McGuire and Hughes' method of edge detection uses a special vertex shader to access the edge mesh data from the vertex buffers prior to doing calculations. Once the data has been obtained, typical object-space edge detection is performed. As mentioned in Section 6.1, the edge tests are:

**Contour**  $(\text{dot}(N_a, V) * \text{dot}(N_b, V)) \leq 0$

**Crease**  $\text{dot}(N_a, N_b) < -\cos(\theta)$

**Boundary**  $v_3 == v_0$

**Marked**  $v_3 == v_0$

Where  $N_a$  and  $N_b$  are calculated:

$N_a = \text{normalize}(\text{cross}((v_1 - v_0), (v_2 - v_0)));$

$N_b = \text{normalize}(\text{cross}((v_3 - v_0), (v_1 - v_0)));$

And  $V$  is calculated:

$V = \text{normalize}(\text{CameraPosition} - v_0);$

In the event that an edge is determined drawable, the vertex shader must calculate an output vertex. McGuire and Hughes differentiated ridge and valley creases. However, the author does not differentiate them in his tests.

### 8.3. Edge Creation

The user has several choices for what type of edge to generate, including a rasterized line, full quad, or half quad. For each type of output, the  $i$  value is used to determine which of several output vertices should be generated.

#### ***Rasterized Line Edge***

For rasterized lines, only two duplicates per edge vertex are needed in the edge mesh. If available, it's most efficient to use an index buffer that contains only the indices of the first two edge vertices per set in the edge mesh. When the  $i$  value is 0, the vertex shader should output  $MVP * v_0$ . Otherwise, it should output  $MVP * v_1$ . MVP is the ModelViewProjection matrix.

#### ***Required Screen-Space Values***

For both quad edge types, McGuire and Hughes create them in screen-space to ensure a consistent thickness. The screen-space versions of some edge components are needed to accomplish the creation process. Those values are:

- $s_0 - v_0$  in screen-space
- $s_1 - v_1$  in screen-space
- $m_0 - n_0$  in screen-space
- $p$  - normalized perpendicular vector to the screen-space edge vector ( $s_1 - s_0$ )

The calculation of each value is described below. Note that the uncommon vector-vector multiplication and division operations are used in these and following operations. They should simply be treated as component-wise multiplication and division. Also note that McGuire and Hughes did not fully convert vertices to screen-space, doing their calculations in projection-space instead. The author fully converts all edge generation vertices and vectors to screen-space in his calculations below.

```
vec4 s0 = MVP * vec4(v0.xyz, 1.0);  
s0.xy = (s0.xy / s0.w) * vec2(Width, Height);  
vec4 s1 = MVP * vec4(v1.xyz, 1.0);  
s1.xy = (s1.xy / s1.w) * vec2(Width, Height);
```

s0 and s1 are calculated storing v0 and v1 multiplied by the combined model, view, and projection matrices (MVP). Then, their x and y components are sent to screen-space by doing the homogeneous division and multiplying by the width and height of the viewport (Width and Height), respectively.

```
vec4 temp = MVP * vec4(v0.xyz + n0.xyz, 1.0);
temp.xy = (temp.xy / temp.w) * vec2(Width, Height);
m0 = normalize(temp.xy - s0.xy);
```

A point on n0 is converted to screen-space, then that value is subtracted from the s0 point. This normalized vector is m0.

```
p = normalize(vec2(s0.y - s1.y, s1.x - s0.x));
```

The p vector can optionally be lengthened or shortened to vary the screen-space thickness of the final quad. Using it and the other screen-space values in conjunction with each vertex's i value, the full and half quads can be created as described below.

**Full Quad Edge**

By default, an edge should be created as a full quad. This always applies to crease, border, and marked edges. Contour edges can optionally be rendered as half quads. The creation of each output vertex is described by the table below.

ID	Output Vertex
i = 0	vec4((s0.xy - p.xy) / vec2(Width, Height) * s0.w, s0.zw)
i = 1	vec4((s1.xy - p.xy) / vec2(Width, Height) * s1.w, s1.zw)
i = 2	vec4((s1.xy + p.xy) / vec2(Width, Height) * s1.w, s1.zw)
i = 3	vec4((s0.xy + p.xy) / vec2(Width, Height) * s0.w, s0.zw)

This output is described graphically in Figure 8-2. Note that the projection to screen-space operation is inverted after offsetting the edge points by the p vector, so that the vertex shader exports valid data.

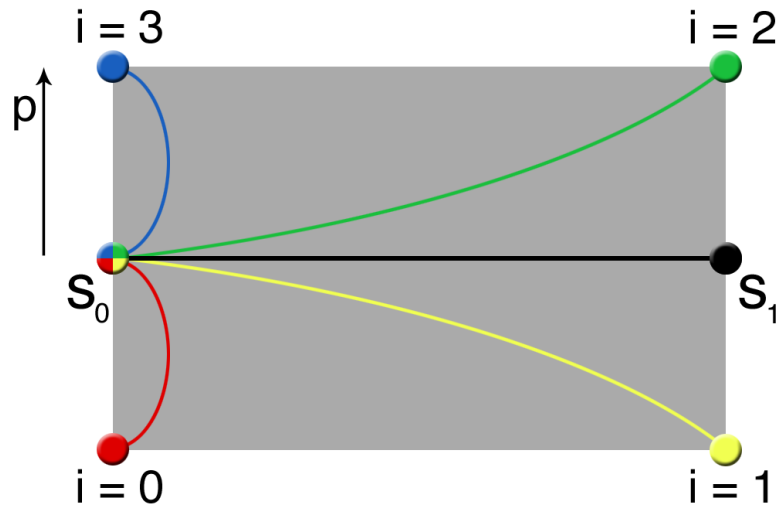


Figure 8-2: For each point in the degenerate set, the output is created based on the  $i$  value.

### Half Quad Edge

The half quad method is intended for use with contour edges only. As mentioned in section 6.3, they prevent the bottom half of the quad from sticking through nearby geometry. To ensure that the edge is rendered to the outside of the mesh, each use of the  $p$  vector is modified by a sign operation. It reverses the direction of  $p$  if it is pointed away from  $m0$  (that is, the angle between them is greater than 90 degrees). The creation of each output vertex is described by the table below.

ID	Output Vertex
$i = 0$	$s0$
$i = 1$	$s1$
$i = 2$	$\text{vec4}((s1.xy + p.xy * \text{sign}(\text{dot}(m0, p)))) / \text{vec2}(\text{Width}, \text{Height}) * s1.w, s1.zw)$
$i = 3$	$\text{vec4}((s0.xy + p.xy * \text{sign}(\text{dot}(m0, p)))) / \text{vec2}(\text{Width}, \text{Height}) * s0.w, s0.zw)$

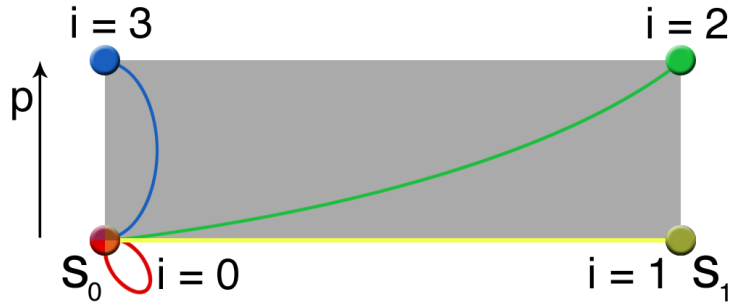


Figure 8-3: The  $p$  vector is always pointing outward in this method, so the edge quad will only render on the outside of the mesh.

### Non-Drawable Edges

If the edge is not drawable, the vertex  $(0, 0, -1, 1)$  should be generated as output. Such a projection-space point will always render behind the near plane, and the pipeline will clip it before attempting to render it. This is how McGuire and Hughes accounted for the vertex shader's inability to delete undesired vertices from the pipeline.

## 8.4. Cap Creation

As mentioned in sections 6.4, when edges are rendered thicker than a few pixels visible gaps occur. To fill them, McGuire and Hughes created caps that render on both sides of each drawn edge. These two half caps are triangle polygons that meet up along the screen-space projection of the shared vertex normal. Two extra render passes are required to create the caps: one for the  $v_0$  side and one for the  $v_1$  side. The caps can be generated from the same edge mesh data as the edges, but they need a different index array buffer. The cap index array buffer needs index values that reference only the first three duplicates of each set of edge vertices.

Unlike the half quad edge method, the caps need to be generated relative to the normal of the vertex to which they are attached. Thus, the screen-space projection of the  $n_1$  vector,  $m_1$ , is also needed to generate the  $v_1$  cap.

It is created:

```
vec4 temp = MVP * vec4(v1.xyz + n1.xyz, 1.0);
temp.xy = (temp.xy / temp.w) * vec2(Width, Height);
m1 = normalize(temp.xy - s1.xy);
```

With m1 and previous screen-space values, the v0 and v1 side half caps are generated as described by the tables below.

ID	Output Vertex (v0 side cap)
i = 0	s0
i = 1	vec4((s0 + p * sign(dot(m0, p))) / vec2(Width, Height) * s0.w, s0.zw)
i = 2	s0 + m0

ID	Output Vertex (v1 side cap)
i = 0	s1
i = 1	vec4((s1 + p * sign(dot(m1, p))) / vec2(Width, Height) * s1.w, s1.zw)
i = 2	s1 + m1

If the user decides to change the edge thickness by scaling the p vector, the m0 and m1 vectors must be scaled by the same amount. McGuire and Hughes were careful to generate the caps in an order that causes only front-facing polygons to occur. The author does not use back-face culling, so this detail was ignored.

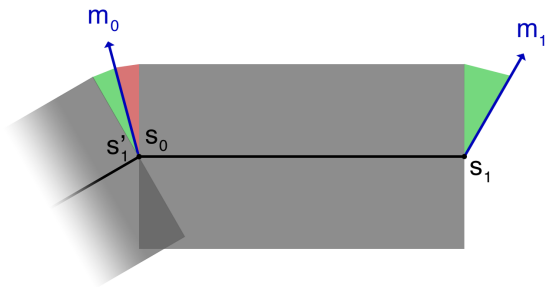


Figure 8-4: Depiction of how caps are formed. The red cap is created for the v0 point. The green caps are created for the v1 point of each drawable edge. Note that two half caps are created for each drawable edge, even if there is no connecting edge. Caps connect along the normal, making them seamless.

## 8.5. Problems

McGuire and Hughes' technique has a few major problems, two of which were caused by the limitations of the hardware available at the time of writing. The author's research was focused on solving these problems.

### ***Screen-Space Thickened Edges***

While it is trivial to scale the thickness of the drawn edges and caps, the use of screen-space scaling makes all edges have the same thickness no matter their distance from the camera. This can cause artifacts and confusion about the distance of the object. Though screen-space thickness may be desired, having a depth-based scaling factor is beneficial for other graphical requirements.

### ***Caps Sometimes Appear on the Wrong Side***

When the screen-space projection of the vertex normals does not correspond well to the curvature of the edge, caps can be generated on the wrong side of the edge under certain perspectives. McGuire and Hughes suggested rendering caps on both sides of the edge when the error is likely to occur.

### ***High Duplication of Work***

The edge detection must occur ten times for all polygon edges: four for the edge, and two sets of three for the half caps. After an edge/cap is determined drawable, the screen-space values must also be generated ten times. Geometry shader usage was proposed as a solution to this problem, but the technology wasn't yet available.

### ***High GPU Memory Usage***

In order to render the object normally, all of the vertex and normal information is already on the GPU in the form of vertex buffer arrays. Not only does the edge mesh contain four duplicates, but all of the data for each edge vertex is duplicating information already on the GPU. This was done because of the limitations of vertex shaders at the time. Shader access to data textures was proposed as a solution for this problem, but the technology wasn't yet available.

## 9. Miscellaneous Contributions

---

The author's research on improvements to McGuire and Hughes' method proceeded along two tracks: small improvements to individual portions of the technique, and complete replacements that take advantage of OpenCL. In this section, the first track is detailed. The following contributions can be implemented directly within McGuire and Hughes' framework.

### 9.1. Depth-Based Edge Thickness

In McGuire and Hughes' method, all edges and caps were drawn scaled along the screen-space perpendicular vector or one of the screen-space vertex normal vectors. Screen-space scaling gives all drawn edges the same thickness, regardless of distance from the viewer. Additionally, edges extending into the distance will appear to get larger the further away they reach, rather than smaller as one might expect from a 3D scene.

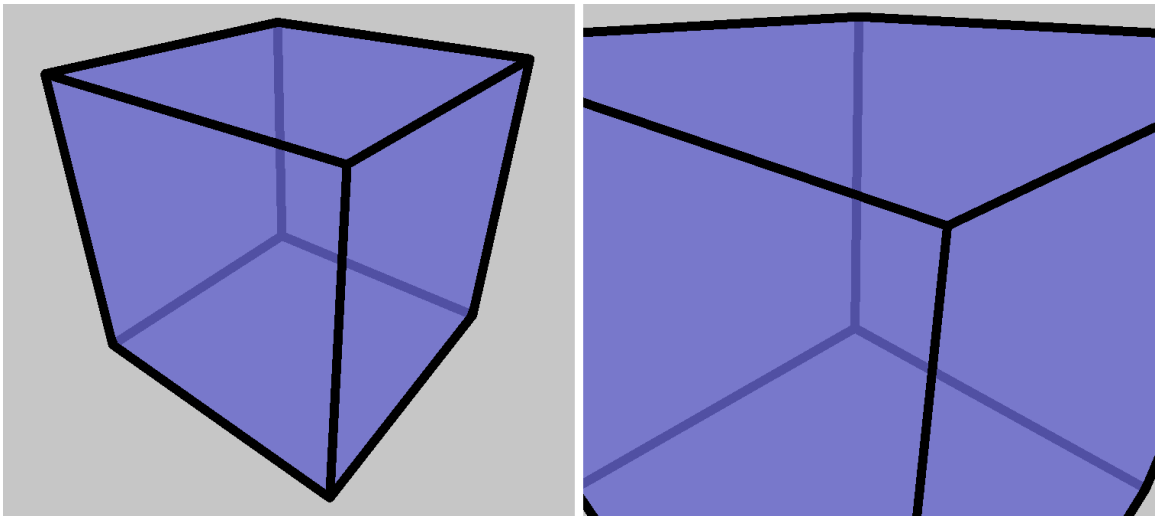


*Figure 9-1: The cube on the left is a few units away from the camera. The right cube's front-most edges are directly in front of the camera, but have the exact same thickness as the cube's back edges.*

Even if these effects are desirable, there is one major disadvantage to this form of scaling. As objects get further from the viewer, the object's geometry will eventually become overwhelmed by the edges.

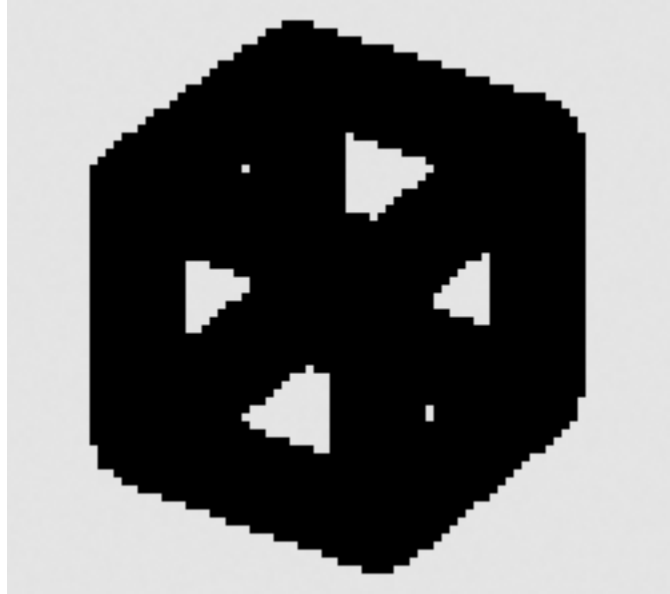


Figure 9-2: This cube is far away from the camera, yet the edges remain the same pixel width, overpowering the mesh.

To allow for more realistically scaled edges and prevent the overpowering problem, the author proposes a depth-based scaling factor be applied to the screen-space perpendicular and normal vectors of each edge vertex.

### ***Naïve Method***

The view-space z-coordinate represents the depth value needed to scale the screen-space vectors realistically. With each vertex in local-space, the naïve method to find their view-space representations uses a matrix multiplication. Then the z-coordinates can be inverted and negated to form the depth-based scaling factor:

```
depthScalingFactor = 1.0 / -(ModelViewMatrix * localSpaceVertex).z;
```

This depth-based scaling factor must be multiplied into each use of the screen-space vectors during the vertex output process, as with any other scaling factors.

### ***Optimized Method***

There is a way to avoid the matrix multiplication entirely. In the process of creating these edges, the projection-space version of  $v_0$  and  $v_1$ 's z-coordinates are created. The depth value at each vertex in the edge can be calculated by multiplying the projection-space z-coordinates by the portions of the inverse projection matrix that apply to z-coordinates.

The inverse projection matrix is:

$$\begin{bmatrix} \frac{r}{n} & 0 & 0 & 0 \\ 0 & \frac{t}{n} & 0 & 0 \\ 0 & 0 & 0 & -1 \\ 0 & 0 & \frac{n-f}{2nf} & \frac{n+f}{2nf} \end{bmatrix}$$

In relation to the z-coordinate, the matrix multiplication operation of the inverse projection matrix and a projection-space point becomes:

$$\text{depth} = 0 * (\text{projected.x} + \text{projected.y} + \text{projected.z}) + (-1 * \text{projected.w});$$

$$\text{depth} = -\text{projected.w};$$

Thus the depth scaling factor calculation becomes:

$$\text{depthScalingFactor} = 1.0 / \text{projected.w};$$

Where projected represents either v0 or v1 in projection-space.

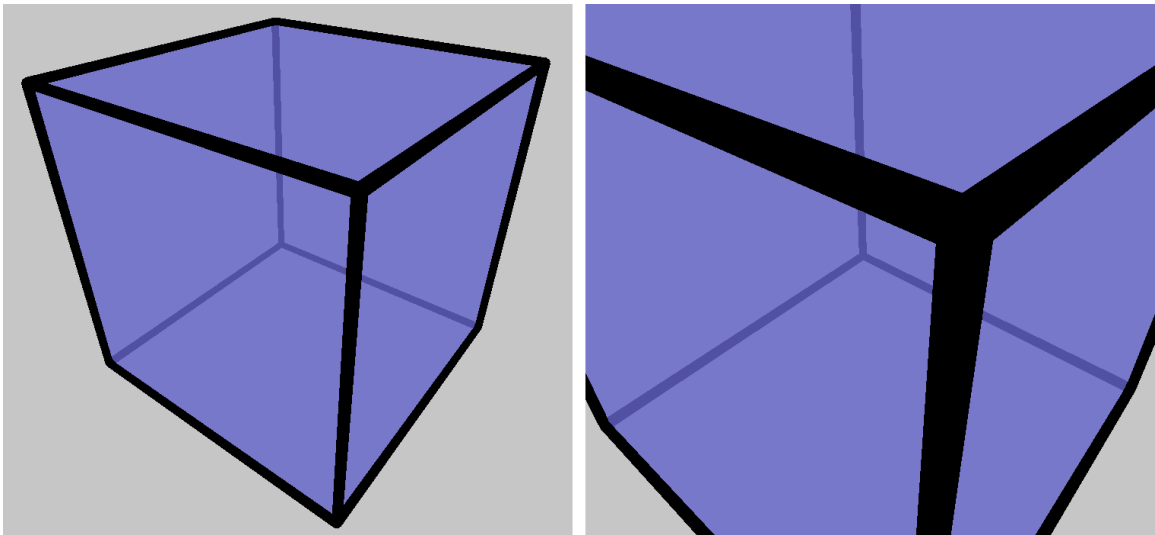


*Figure 9-3: The same cube as above with the depth-based scaled thick edges. Notice how each edge's thickness will scale along its length.*

### ***Orthographic Projection Considerations***

Such a compact optimization is not available when using orthographic projection. After applying the same rules to the inverted orthographic projection matrix, the calculation becomes:

```
depthScalingFactor = -2.0 / (projected.z * (n - f) - projected.w * (n + f));
```

The amount of calculation is not significantly less than accessing the value through world-space vector multiplication with the ModelView matrix, and requires two additional pieces of data: the near and far plane distances (n and f).

### ***Minimum Thickness***

One final improvement to the thickness modification is to cap the bottom of the scale factor through the use of a max function. This will assure a minimum edge thickness no matter the distance of the object.

```
depthScalingFactor = max(1.0, 1.0 / projected.w);
```

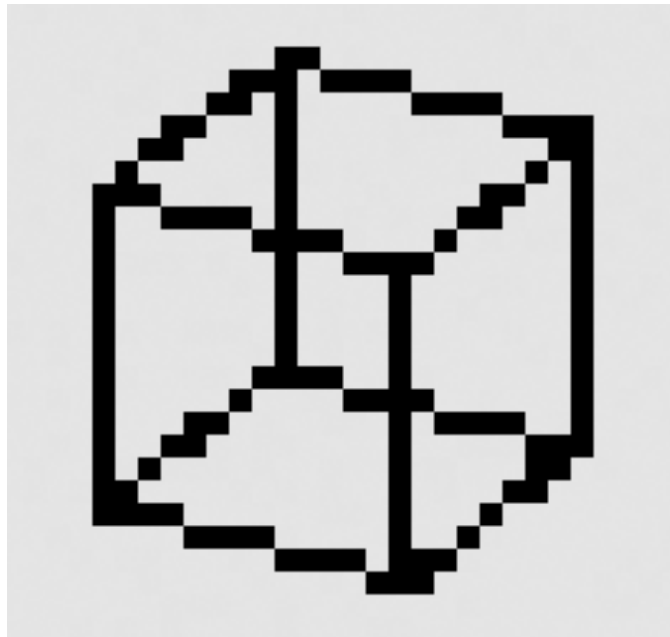


*Figure 9-4: A distant cube with edges that remain visible yet do not overpower the mesh.*

Edges rendered with a minimum thickness of less than one can cause flickering and missing edges if the distance is great enough.

## 9.2. Reduce Effects of Incorrectly Projected Normals

The screen-space projection of each vertex's normal is used to choose the side on which to render the caps. For some meshes viewed from certain view angles, the projected normals will point in the wrong direction, causing caps to appear on the wrong side of the edge. McGuire and Hughes suggested that the caps be rendered on both sides of the edge in cases where this might occur.

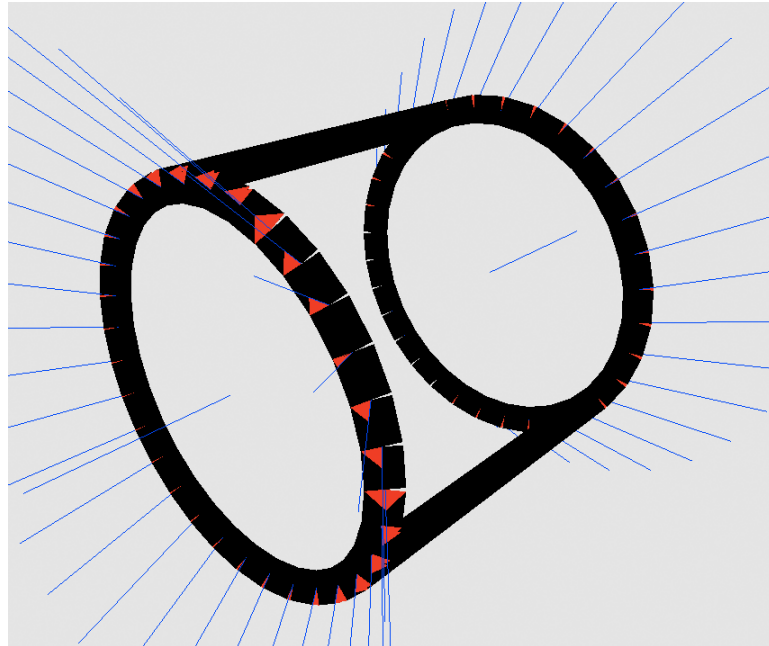


*Figure 9-5: The shared vertex normals (blue) of the cylinder crease edges, when viewed from this angle, demonstrate the failure case of normal-based capping (red).*

The author found that for every potential gap created at the intersection of two drawable edges, there is exactly one “normal” vector that, when projected, would yield a correctly placed cap. Each vertex is limited to a single normal vector because of the restriction to only include unique edges. However, if edges are defined not only by their location, but also by their normals, the problem can be solved. Crease edges tend to have more than one appropriate normal, as indicated in McGuire and Hughes’ paper. By using a common crease splitting operation in a 3D application, and allowing edges to be distinguished by their normals in addition to their position, some edges are duplicated, but with appropriate normals. This is a simple application of the proposed solution in McGuire and Hughes’ paper.

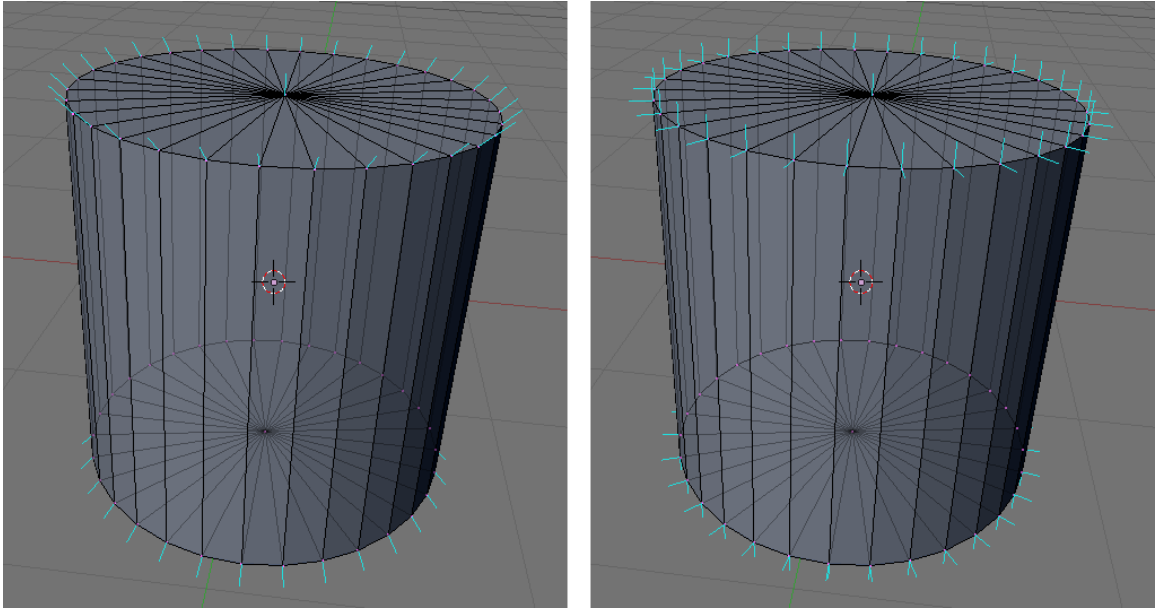


*Figure 9-6: The shared vertex normals of the left cylinder generate caps that end up on the wrong sides from some view angles. The right cylinder, which has appropriate normals for each major section of the mesh at the cost of duplicate edges, will generate correct caps no matter the view angle.*

If the right cylinder from figure 9-6 is rendered, the output looks like Figure 9-7. Since the edges are created without the normals, any duplicate edges could be marked to output a degenerate edge quad. The cap creation would remain the same. Doing this would reduce the impact of having the additional edges in the edge mesh. Using caps on both sides for all crease edges would yield similar results, but at the cost of additional render passes.

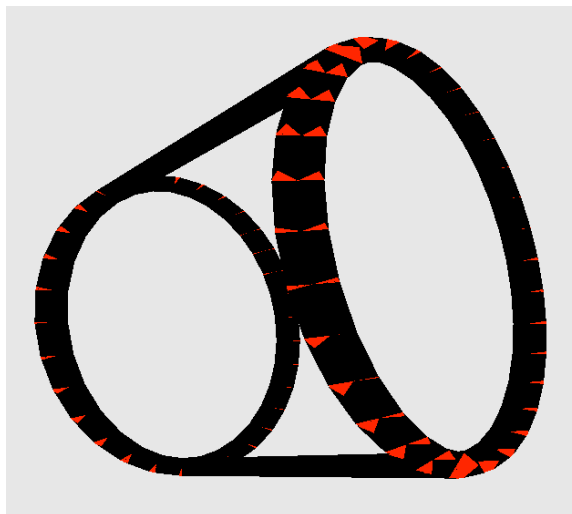


*Figure 9-7: A second set of normals for problematic edges generates the correct output.*

For some meshes, the problematic normals originate from a curved portion of the mesh abutting a flat portion. When these objects are created, the vertices that connect the curved and flat portions get blended normals, which are incorrect for both portions (see Figure 9-6). Flat portions of meshes, as long as they are connected at their extreme edges to a non-flat surface, should not generate edges at all. Therefore, their normals should not influence the edge detection of other edges. For a cylinder, the correct normals on the ends are the same as the normals for a tube.

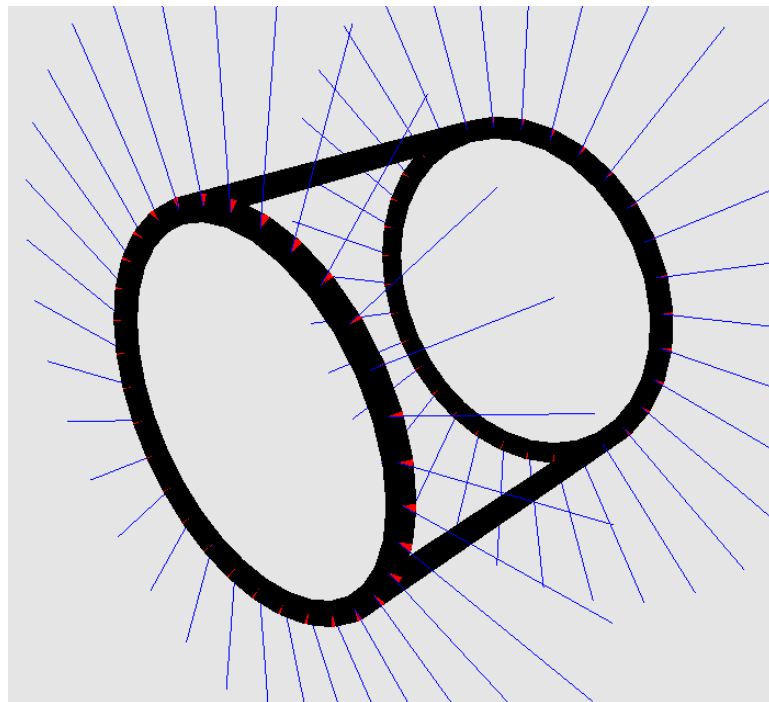


*Figure 9-8: The tube's normals create the perfect normals for a cylinder. No matter the view angle, the normals of the flat surface were not needed to generate the correct caps.*

Unfortunately, the flat to curved abutment is not the only case that will cause problems when the normals are projected. For example, when a plane is created, many 3D applications create the normals so that they all point upward out of the plane. However, to generate the appropriate caps for the boundary edges of the plane, the normals should lie on the same plane as the mesh itself, pointing diagonally outward.

Although the author was unable to find an algorithmic solution to generate appropriate normals for every kind of mesh at every view angle, he did find that

the correct cap could always be generated with enough edge duplicates or a better normal chosen by a discerning eye.

### 9.3. Alternate Drawable Edge Types

The author explored several methods to reduce the amount of duplicate edge tests and other calculations by combining multiple passes together. The resulting new edge structures have various advantages and disadvantages over McGuire and Hughes' edge/cap drawing method. All of these new edge types render slightly faster than McGuire and Hughes' edges.

#### ***Half Hex Edges***

Half hex edges combine the area of a half quad edge and the two half caps. They form a hexagon shaped edge on the "outside" of the mesh out of two quads. This combination eliminates one whole render pass, and reduces the number of output vertices needed by two.

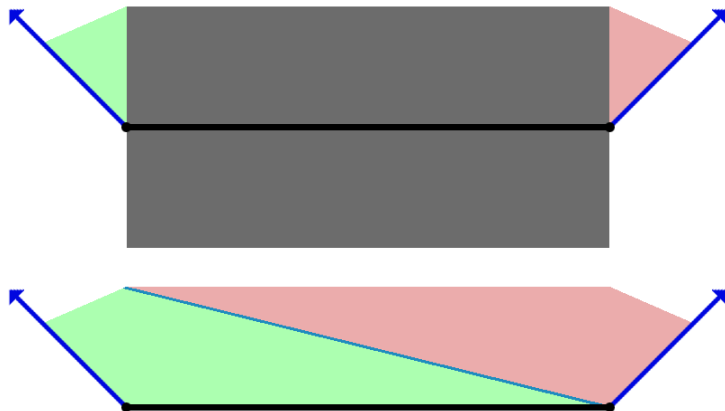


*Figure 9-9: McGuire and Hughes' edge and two half caps setup (top) compared to a half hex edge (bottom). The blue arrows represent the vertex normals for the black edge. The half hex edge combines the caps into the edge, but is only rendered on the "outside" of the mesh.*

The area in half hex edges, as with other other alternate edges, can be split into quads in multiple ways. For the sake of simplicity, only the split method displayed in the figure above will be used to describe the output vertices.

ID	Output Vertex (green side)
i = 0	s0
i = 1	s1
i = 2	$\text{vec4}((s0.xy + p.xy * \text{sign}(\text{dot}(m0, p)))) / \text{vec2}(\text{Width}, \text{Height}) * s0.w, s0.zw)$
i = 3	$\text{vec4}((s0.xy + m0.xy) / \text{vec2}(\text{Width}, \text{Height}) * s0.w, s0.zw)$

ID	Output Vertex (red side)
i = 0	$\text{vec4}((s0.xy + p.xy * \text{sign}(\text{dot}(m0, p)))) / \text{vec2}(\text{Width}, \text{Height}) * s0.w, s0.zw)$
i = 1	s1
i = 2	$\text{vec4}((s1.xy + m1.xy) / \text{vec2}(\text{Width}, \text{Height}) * s1.w, s1.zw)$
i = 3	$\text{vec4}((s1.xy + p.xy * \text{sign}(\text{dot}(m0, p)))) / \text{vec2}(\text{Width}, \text{Height}) * s1.w, s1.zw)$

Half hex edges only render on the side of the m0 vector. Thus they are only suitable for use with contour edges. Noticeable edge flipping occurs if they are used for other types of drawable edges.

### ***House Edges***

House edges are named for their silhouette. They have a large base that extends above and below the polygon edge, and a “roof” that sits on top of the base.

House edges require two new vertices not seen in other drawn edge types. They are the intersections of a line and two vectors. A special perpendicular vector is required for these calculations:

```
pAlt = p * sign(dot(p, m0));
```

The line is defined by two points:

```
innerS0 = s0 + pAlt;
```

```
innerS1 = s1 + pAlt;
```

The two vectors are two instances of the altered perpendicular vector, with origins at each of the screen-space normal offset vertices:

```
p0originPoint0 = s0 + m0;
```

```
p0originPoint1 = s1 + m1;
```

The two additional vertices are calculated using the standard 2D intersection formula between vectors and a line. The other four vertices are calculated as in other techniques. They include: s0 offset by m0, s1 offset by m1, s1 offset by the “outward” p vector, and s0 offset by the “outward” p vector. See Figure 9-10 for a visual depiction of a house edge.

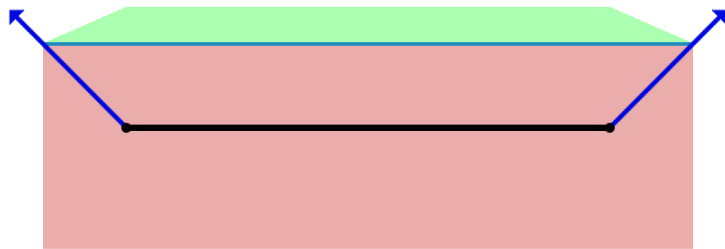


*Figure 9-10: The house edge extends downward from the normal-offset points until the bottom of the inside edge is reached. This type of drawn edge covers much more area than other types.*

The house edge generates very bad artifacts at even remotely sharp connecting edges. The extra area on the underside makes the problem of thick edges passing through nearby geometry even worse. This type of edge is not recommended for use in any circumstance, despite its slightly higher speed compared to McGuire and Hughes’ method.

### **Plug Edges**

Plug edges, also named for their silhouette, combine the good qualities of half hex and the house methods. It uses only two passes, generates area on both sides of the edge, and doesn’t create too much extra area. It also creates only output vertices used in McGuire and Hughes’ edges, so the terrible artifacts of the house method are non-existent.

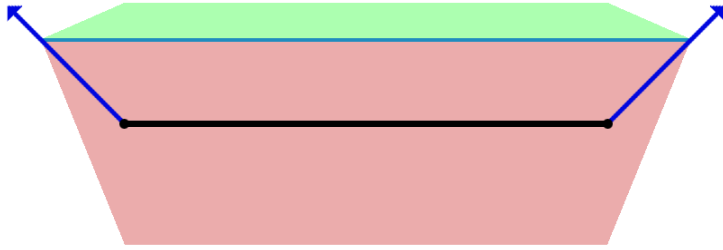


*Figure 9-11: The plug edge takes the idea of the house edge, but simplifies it so that the points at the bottom match up with the actual extended edge point (vertex - perpendicular). This edge method generates a lot less area than the house edge, but retains the edge/cap combination.*

Plug edges can be used for crease and boundary edges, while half hex edges can handle the contours. This combination generates quality roughly equivalent to McGuire and Hughes' edge/caps, but with the speed advantage of only two passes per mesh.

## 10. Non-Duplicate Parallel Edge Detection and Capping

---

After researching and implementing McGuire and Hughes' method, the author focused on improving it. The most extensive research focused on finding a replacement technique that would take advantage of the new capabilities of OpenCL. The main alternative technique discovered is called non-duplicate parallel edge detection and capping.

OpenCL (Open Computing Language) is a framework for doing general computation on a wide variety of hardware. It's primary focus is to unlock the massively parallel computational power of modern GPUs for non-graphical applications. It also offers buffer interoperability with OpenGL (Open Graphics Library). The author discovered that these features lend themselves well to object-space edge detection. It single-handedly replaces the two future technologies mentioned in McGuire and Hughes' paper as ways to improve their method: geometry shaders and data texture lookup. Simultaneously, it provides a way to create more accurate caps by eliminating the problem of inappropriate normal projection.

### 10.1. Method Overview

OpenCL allows the reading and writing of OpenGL vertex buffers. This means that the geometric and connectivity data need not be sent to the OpenCL context every frame. It can be generated during a preprocessing step and then transferred to the GPU's buffers, just as McGuire and Hughes did. Unfortunately, OpenCL does not support rendering commands, so detection and rendering must be separate steps.

Since all vertex buffers on the GPU are theoretically available to an OpenCL program (called a kernel), duplicate vertex information is not needed. The kernel can make use of the mesh's vertices already on the GPU. The only additional buffer needed for edge detection is the vertex connectivity information in the form of vertex indices. By not repeating 3D vertex information, the amount of extra

data required to detect edges is significantly lower than in McGuire and Hughes' method.

Once the data is retrieved, the edge detecting step is largely the same as in McGuire and Hughes' method, with two exceptions: edge detection and edge value generation occurs once per edge, and the output vertices are stored to an output buffer rather than being rendered directly.

The caps, on the other hand, are created completely differently from McGuire and Hughes' method. The cap creation kernel uses output data from the edge detecting step to completely skip the edge detection step in each cap. Normals are not used in the creation process, so caps no longer appear on the wrong side of the edge under any circumstance.

Edges and caps both require one calculation pass. Then three very simple rendering passes render the mesh, edges, and caps. The details of the implementation are below.

## **10.2. Data Structure**

A large amount of preprocessing is required to arrange a mesh's polygon edges into the edge and cap meshes. The edge mesh is similar to the one generated for McGuire and Hughes' method, except that only the connectivity information is needed in the form of indices. Only one set of indices are need per edge, rather than four in McGuire and Hughes' method.

The cap mesh, however, indexes into the edge mesh. A cap vertex in the cap mesh contains a reference to the two connecting edges. Since all edges output a quad, even if degenerate, it is trivial to obtain information about each edge's state of drawability.

First, all triangles in the mesh are processed to generate a list of unique edges with associated adjacent points. Since indices are being used instead of the actual data, each edge vertex contains:

- Edge vertex index 0 (indexes the vertex buffer)
- Edge vertex index 1 (indexes the vertex buffer)

- Adjacent vertex index 0 (indexes the vertex buffer)
- Adjacent vertex index 1 (indexes the vertex buffer)

All of these edge vertices together represent the edge buffer. These indices refer to the vertex buffer for the mesh, and could also be used to access the normals. As with McGuire and Hughes' method, if the adjacent vertex index 1 does not exist because the edge is a boundary edge, it is set equal to edge vertex index 0.

Another buffer, the edge out buffer, needs to be created with enough space to contain the set of four potential projection-space output vertices for each edge in the edge buffer. The buffer must have room for  $4E$  four dimensional vertices, where  $E$  is the number of edges in the edge buffer. This buffer will hold the quad representations of the drawable edges for the dual purpose of rendering edges and defining which caps should be drawn.

Then the cap buffer should be created, using the edge and vertex buffers' indices. Each cap vertex contains:

- Edge index 0 (indexes the edge buffer)
- Edge index 1 (indexes the edge buffer)

As with the edge buffer, the cap buffer needs a corresponding cap out buffer to store its sets of projection-space vertices for later rendering. Since these caps will be made of quads, the buffer must be able to store  $4C$  four dimensional vertices, where  $C$  is the number of caps in the cap buffer.

Once all these buffers have been created, and the two input buffers populated, they should be sent to the graphics card in preparation for edge detection and rendering. Refer to Figure 10-1 for a depiction of the buffers' relationships.

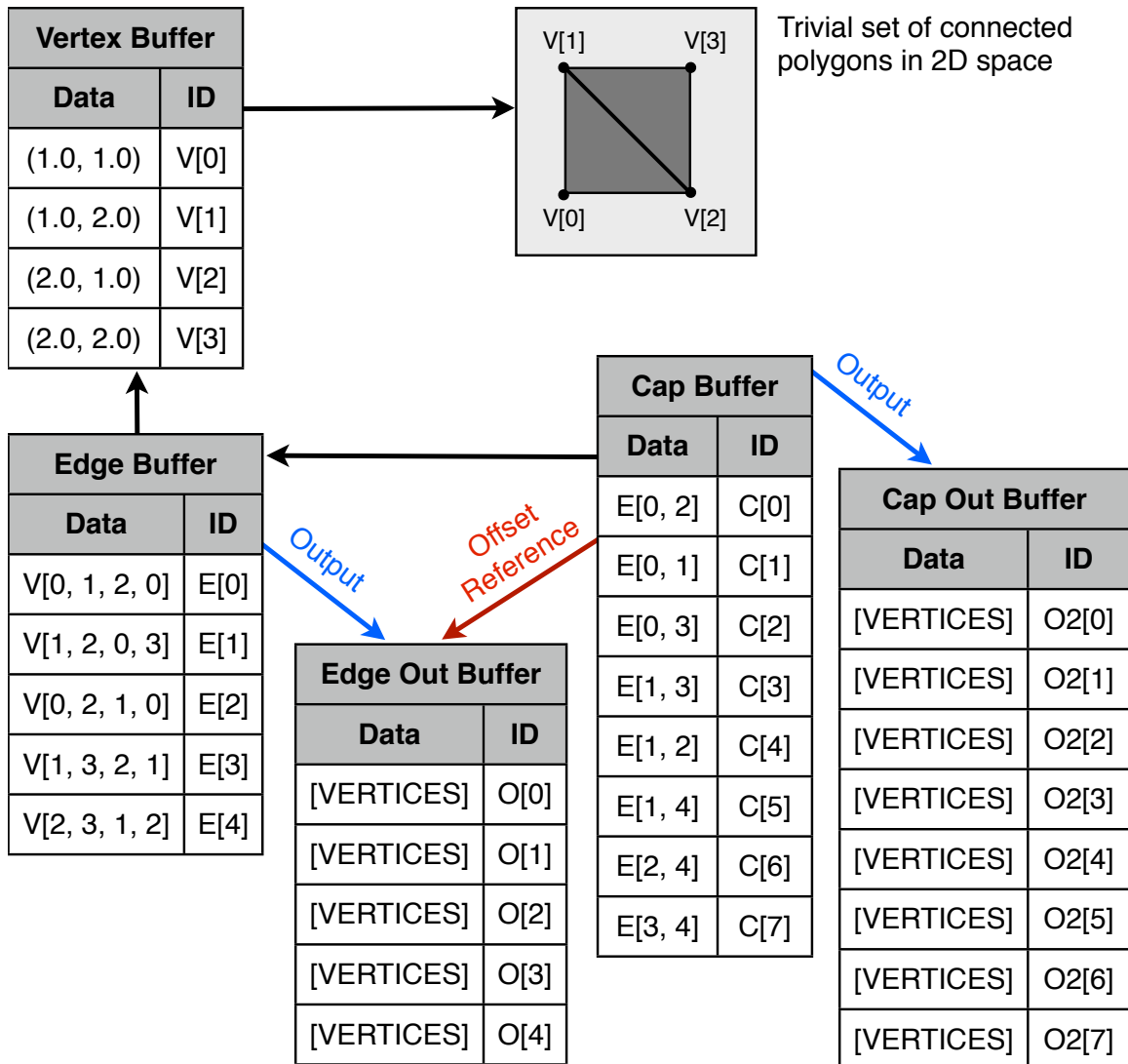


Figure 10-1: For a trivial set of polygon edges (top), the vertex buffer is used with the index buffer (not shown) to draw the mesh normally. The edge vertices (edge out buffer) are calculated using the edge buffer which contains vertex connectivity information referring to indices of the vertex buffer. The edge connectivity information (the two edge buffer indices in the cap buffer) are used to offset index into the edge out buffer where drawability is easily determined. If the cap should be drawn, the cap out buffer is filled with cap vertices by using the cap buffer's two edge buffer references to determine the point of contact and how to draw the cap.

### 10.3. OpenCL Notes

OpenCL can only access OpenGL buffers if the context of OpenCL is initialized with OpenGL's context. Obtaining the OpenGL context is implementation-specific. Once obtained, all OpenGL buffers in the context can be read freely. In order to write to them, however, OpenCL must acquire or lock those buffers prior

to operating on them. In order for OpenGL to regain the ability to render from those buffers, they must be released from OpenCL.

Additionally, non-texture buffer access of OpenGL buffers by OpenCL use the uncached global GPU memory. This memory access is very slow, so optimization is very important to achieving good results. Accessing several values of adjacent global memory should be done via the vector load and store functions. This reduces the overall memory calls significantly. Functions for manual data caching can alleviate most memory access speed issues, though some algorithms do not lend themselves well to their use.

Several other OpenCL specifics affect speed. Data transfer from the CPU to the GPU is very costly and should be avoided as much as possible. Doing a high number of calculations in OpenCL is required to offset the speed loss of the transfer. If the data is already on the graphics card, and the results of the calculation remains on the graphics card, as with the author's algorithm, this transfer penalty is not felt.

Having logical forks (if statements) in a kernel slows down the processing of all threads, because code in the kernels are executed in lock-step. If one set of threads enters the if statement, all the threads that would enter the else statement are blocked until the other threads are finished with their if statement code.

#### **10.4. Edge Detection and Creation**

When the user activates the OpenCL edge detection kernel, the user supplies the number of threads it will perform. That quantity should be the number of edges in the edge buffer. While running, each thread's kernel has the ability to ask for its ID within all threads. This ID is used as the index for the edge buffer.

In addition to the kernel ID, the edge detection kernel requires references to the vertex, edge, and edge out buffers and copies of the ModelViewProjection matrix, the camera position, and the viewport width and height. The four vertex buffer indices obtained from the edge buffer are then used to obtain the vertices

necessary for edge detection: the two vertices defining the edge, and the vertices defining the adjacent points on the two connected polygons. This information is exactly the information available to McGuire and Hughes' shaders at the time of edge drawability testing.

The actual edge detection steps are exactly the same as those in McGuire and Hughes' method, with the minor exception that boundary and marked edges can be checked for drawability using index comparisons instead of vertex comparisons. Check section 8.2 for the details.

For edges that are drawable, the kernel should generate the screen-space values necessary to generate the quad edge and then send those four vertices to the edge out buffer. These values should be exported in projection-space, just as the vertices were output from McGuire and Hughes' vertex shaders. At this point, all four vertices can be generated in one step, preventing a lot of duplicate computations. As with detection, the edge creation process is identical to that of McGuire and Hughes' method (section 8.3). For edges that are non-drawable, a degenerate quad made up of the vertex  $(0, 0, -1, 1)$  should be sent to the edge out buffer.

With the edge detection step complete, the edge out buffer contains sequential quad vertices that define the drawable edges. Non-drawable edges have degenerate quad entries that will be clipped during the rendering process.

## **10.5. Cap Detection and Creation**

Cap detection is a completely new operation. In McGuire and Hughes' method, two half caps were created on each side of every drawable edge. Since the cap buffer provides the connectivity information of every possible combination of connecting edges, the caps can be generated more accurately.

Like the edge detection step, the cap kernel will need some of the same resources including, but not limited to: references to the edge, edge out, cap, and cap out buffers and a copy of the viewport width and height. The number of cap kernel operations should be equal to the number of entries in the cap buffer. The

cap kernel supplies an ID that can be used to index into the input and output buffers, as was done in the edge detection kernel.

Each vertex in the cap buffer contains indexes to the two connecting edges of each cap. The cap data can be used to obtain the indices of the two edges, and those can be used to obtain the original edge vertices. Then a typical edge test could be performed to determine the drawability of both of the edges. However, it's more efficient to use the recently populated edge out buffer to determine the drawability state of both of the connecting edges.

All non-drawable edges generate a degenerate quad made of the vertex  $(0, 0, -1, 1)$  in the edge out buffer. Using the indices of the connecting edges, the kernel can obtain the first output vertex of each connecting edge. If both of these output vertices are not equal to the degenerate vertex, they are both drawable and the cap should be created at the connecting vertex. If only one or neither of them are drawable, then no cap should be created. Instead, a degenerate quad made of the vertex  $(0, 0, -1, 1)$  should be stored in the cap out buffer. Alternatively, the vector comparison could be simplified by building the output vertices for degenerate edges from  $(\text{NAN}, 0, -1, 1)$ . This reduces the drawability test to a single value check for equivalence with NAN (or Not A Number).

If the cap is drawable, the kernel must determine the order of the edges so that the relative position of the connecting point and the two outer points are known. The order can be checked by comparing the relative values for each edge index's vertex indices. Then, using the projection-space vertices in the edge out buffer, the screen-space vertices of the edge quads can be calculated. The calculation is done the same way the edges' vertices were sent to screen-space: homogeneous division and scaling by the viewport width and height.

After all the vertices are ordered and in screen-space, three screen-space vertices need to be determined:

- sL - the vertex on "left" edge that is not the connection vertex
- sM - the connecting vertex
- sR - the vertex on the "right" edge that is not the connection vertex

Using the vectors along the edges, the “middle vector” needs to be determined. This vector lies on the same plane as, and points away from, the two edges. The middle vector will be used to generate the connecting point that was previously obtained from vertex normals.

It is calculated:

```
middleVector.xy = -normalize(normalize(sL.xy - sM.xy) + normalize(sR.xy
    - sM.xy));
```

The perpendicular vector for both edges are needed for the rest of the calculation. The “left” edge’s perpendicular vector will be referred to as p0, and the other, p1. They are obtained:

```
p0 = normalize((float2)(sL.y - sM.y, sM.x - sL.x));
```

```
p1 = normalize((float2)(sR.y - sM.y, sM.x - sR.x));
```

They need to be modified to point in the same direction as the middle vector (less than 90 degrees of angular separation). This modification is accomplished via the operations below:

```
p0 = p0 * sign(dot(p0, middleVector));
```

```
p1 = p1 * sign(dot(p1, middleVector));
```

After all these values have been generated, the output vertices for the drawable caps can be sent to the cap out buffer. The vertices of the cap are listed in the table below.

Vertex	Calculation
0	(float4)((sM.xy + middleVector) / sM.w * (float2)(ScreenWidth, ScreenHeight), sM.zw)
1	(float4)((sM.xy + p0) / sM.w * (float2)(ScreenWidth, ScreenHeight), sM.zw)
2	(float4)(sM.xy / sM.w * (float2)(ScreenWidth, ScreenHeight), sM.zw)
3	(float4)((sM.xy + p1) / sM.w * (float2)(ScreenWidth, ScreenHeight), sM.zw)

Since the cap's creation is based on the connected edges rather than the normal, the normal's orientation is irrelevant to the position of the cap. The cap also always perfectly fills the gap created between the two edges, no matter how the two edges are oriented.

An alternative method of obtaining the  $p_0$  and  $p_1$  vectors is to look them up in the set of already determined points from the edge quad. The  $p$  vectors must still point in the direction of the middle vector, however.

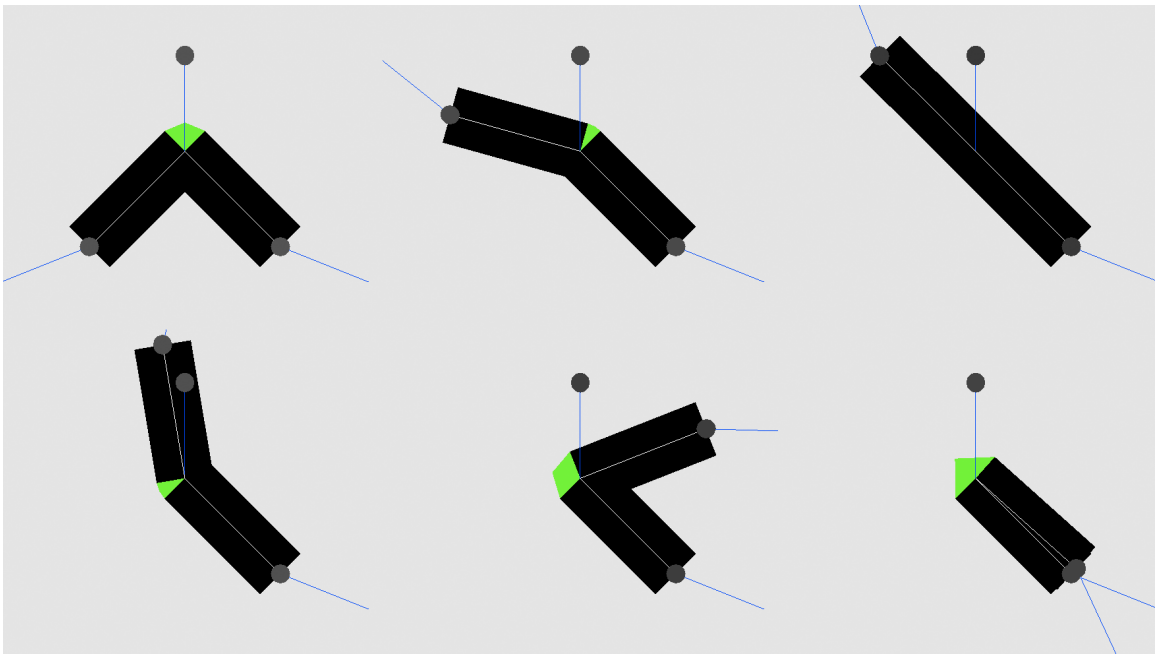


*Figure 10-2: The green caps are generated without the use of the normal, and always perfectly fill the gap between the two edges because they are created utilizing the vertices of both edges.*

If half quad edges were used when creating the edge quads, there is no longer a trivial solution for exactly where the cap should be placed. There are many possible combinations of half and full quads, as orientation relative to the line and the bend of the connection is relevant. Though the correct cap output can eventually be calculated, there is no known elegant solution to determining exactly when and where.

## 10.6. Rendering

All edge and cap vertices were output from their respective kernels in projection-space, the output format of vertex shaders. Thus, the vertex shader for the edges

and caps must only pass the vertex through directly, with no additional processing. The vertex shader is displayed below.

```
void main() { gl_Position = gl_Vertex; }
```

The complete render process consists of rendering the mesh normally, with a slight backwards offset, then rendering the edges and caps as ordered quad arrays. Because OpenCL can interoperate with OpenGL's buffers, no edge, cap, or vertex data is sent to or retrieved from the GPU during each frame.

## 11. Comparative Analysis

---

Having implemented McGuire and Hughes' method and an unoptimized version of the author's method, non-duplicate parallel edge detection and capping, the author was surprised to find that his technique was vastly slower than McGuire and Hughes'.

The author researched the reason for this discrepancy. In order to be assured that it was not an algorithmic issue, the author reimplemented both methods on the CPU, as memory access speed was suspected as the main cause at the time.

The CPU implementations yielded better results, with the author's method running approximately four times faster than McGuire and Hughes' method for complex meshes, as expected. Of course, the faster speed of the author's algorithm on the CPU was not faster than McGuire and Hughes' method on the GPU.

Next, the author wrote an optimized version of his method in OpenCL, taking full advantage of vector loads and stores. Though it led to a significant speedup over the unoptimized version, it remained slower than McGuire and Hughes' method. The sheer number of caps to check and the lack of short-circuiting in non-drawable caps was suspected for the speed problems.

The author then implemented McGuire and Hughes' capping method using OpenCL so that edges and caps would be created in a single pass, with one thread per edge. This led to a dramatic speedup, but except for very complex meshes, it was still slower than the algorithm implemented on the shader. At this point, the suspected bottleneck was the lack of memory caching.

Dr. Xin Li [Li 10] suggested a system to reduce the total number of caps considered. In the process of generating the edge out buffer, a secondary buffer was generated containing only the values one and zero depending on the drawability of that edge. Next, a kernel would simultaneously transform the values equal to one into their edge index value and shuffle them toward the front

of a drawable edges list. After the shuffling was completed, the quantity value of drawable edges was returned to the CPU. The next kernel acted only on the front of the drawable edge list, only processing drawable edges. This kernel generated a valid cap list, where each combination of edges were both connecting and drawable. Another shuffling step shifted all the valid caps to the front of their list and returned the total quantity. Finally, the cap kernel could be run just on valid caps, removing the need to process caps that wouldn't be drawn.

This implementation only reached the framework stage. At that time, it was discovered that, even with the reduction in caps processed, the cost of returning data from the GPU slowed the algorithm down too much to be seriously considered as a solution.

Thus, the author found several methods to implement object-space edge detection using OpenCL, but thus far, none are quite as fast as McGuire and Hughes' method. However, the author's method still retains one advantage over McGuire and Hughes' method: the more accurate cap placement. Implementing McGuire and Hughes' algorithm in OpenCL also significantly reduces the memory usage compared to the shader version.

In this section, the operation quantity, memory access, memory usage, rendering quantity, and overall speed will be compared in the important variations listed above. The section concludes with a description of the various factors that contribute to the overall lower speed of the author's methods. Section 13 contains a few additional suggestions that might lead to further improvements.

### **11.1. Operation Quantities**

In the following two charts, the author displays information on the number of various operations performed in the process of creating edges and caps. These figures are divided further into best/worst case (non-drawable/drawable) scenarios and M&H/Ar (McGuire and Hughes'/author's) methods. These quantities were counted during the CPU implementation. Though other types of implementations will have more or less than these exact quantities, the important

factor is the magnitude of the difference between them, which will not significantly change.

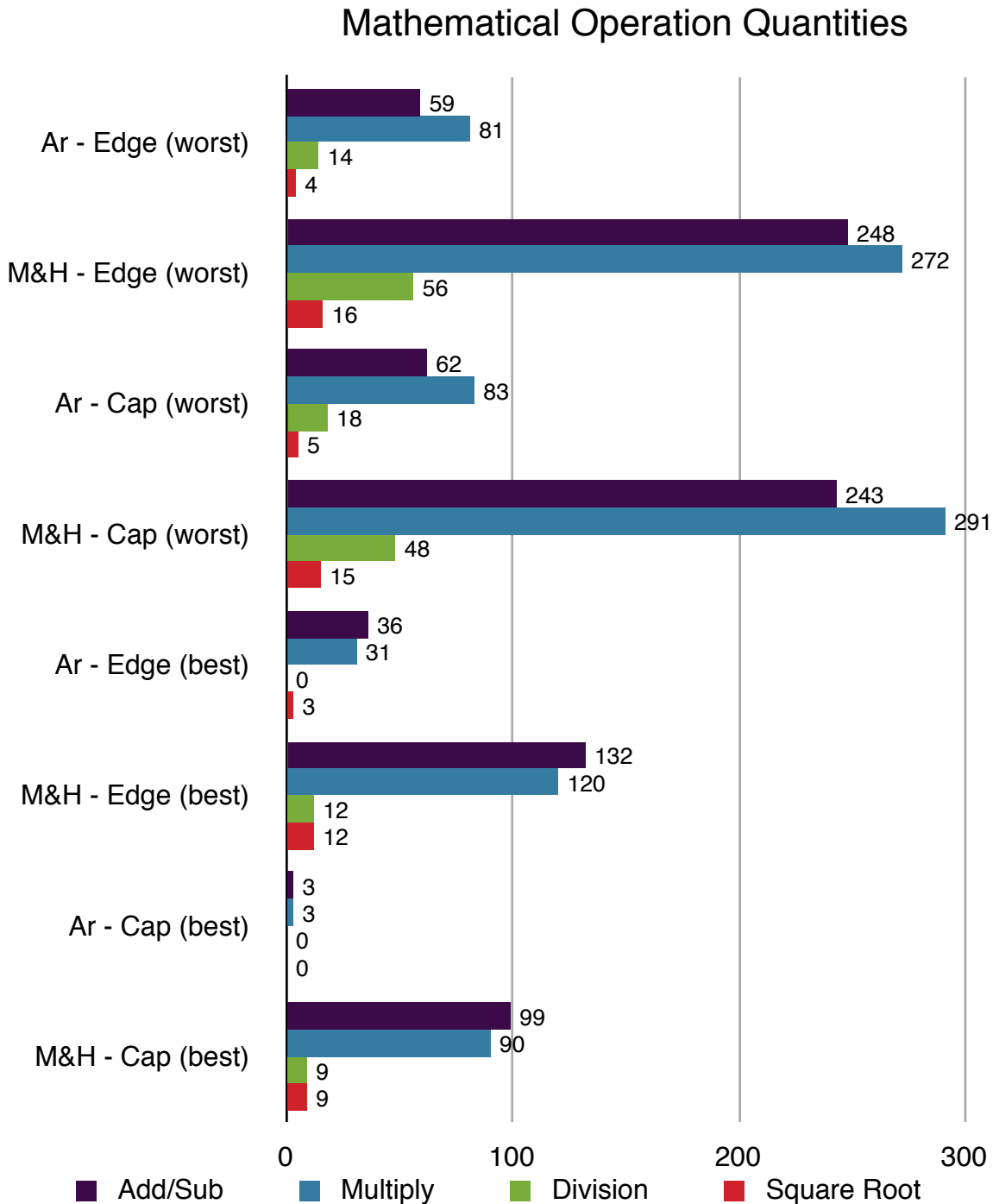


Figure 11-1: This chart shows the relative quantity of different types of mathematical operations used by both methods under different conditions. The author's method has fewer operations overall due to lack of duplication and test optimizations. Smaller is better.

## Logical/Other Operations

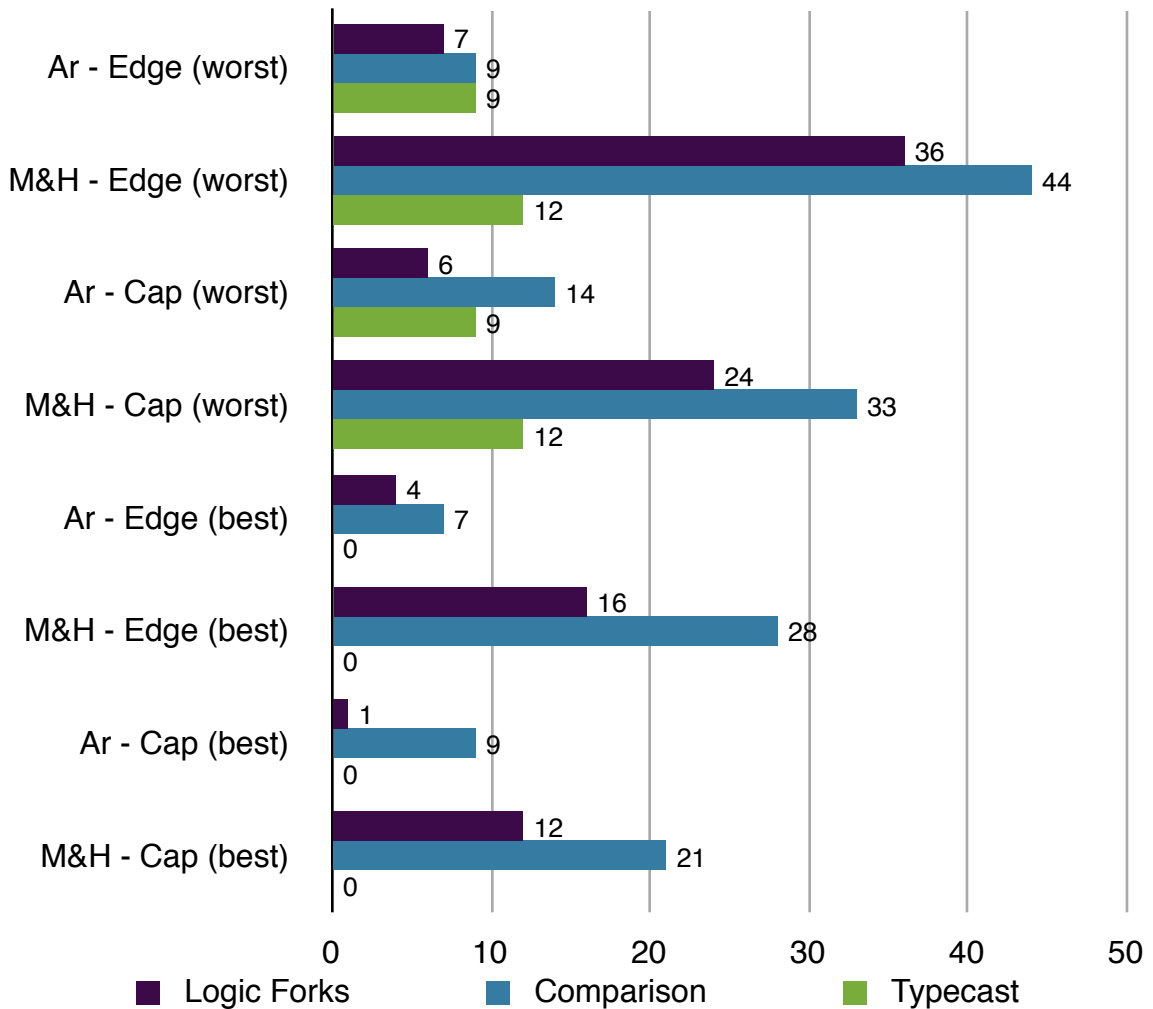


Figure 11-2: This is a comparison of the number of logical forks (if statements), comparison operations, and typecasts (vector types) used by each method under different conditions. The author's method has fewer operations overall due to lack of duplication and test optimizations. Smaller is better.

The following table shows the ratio comparisons of the two methods. While the quantities of all operations were reduced in the author’s method, many of them are from the simple elimination of duplication. Those ratios that represent an operation reduction of greater than four times are displayed with a green cell. Smaller is better.

	Edge Ratio Ar : M&H Worst Case	Cap Ratio Ar : M&H Worst Case	Edge Ratio Ar : M&H Best Case	Cap Ratio Ar : M&H Best Case
Add/Sub	0.238	0.255	0.272	0.03
Multiply	0.298	0.285	0.258	0.033
Division	0.25	0.375	0	0
Square Root	0.25	0.333	0.25	0
Logic Forks	0.194	0.25	0.25	0.083
Comparisons	0.205	0.424	0.25	0.429
Typecasts	0.75	0.75	N/A	N/A

## 11.2. Memory

In this section, GPU memory accesses and usage is compared for edges and caps.

### ***Memory Access***

As previously mentioned, memory access speeds are significantly different for shaders and OpenCL. Shaders get their memory access in a cached form, which makes them significantly faster than access to global memory in OpenCL.

Because the shader memory access is ordered and cached, the number of memory reads and writes are essentially irrelevant to the final speed. In OpenCL, however the number and type of memory accesses is significant. Using vector loads and stores, the number of reads for both edges and caps is five. The number of writes is one for both edges and caps. Edges and caps have no best or worst case in terms of memory access. They always access the same amount of global GPU memory.

In McGuire and Hughes’ method, output data is sent directly into the pipeline for rendering. The author’s method, on the other hand, must store those values to a

buffer for later rendering. This is why both edges and caps must write some data to memory.

If the McGuire and Hughes' method of capping is implemented in OpenCL, a single kernel creates both the edge and the two end caps. This edge/cap combination uses seven global memory reads and three memory writes.

### ***Memory Usage***

Calculating the total memory footprint of both edges and caps is dependent on the number of possible edges and caps, the view direction, and the type of mesh in question. So, several tables are needed to illustrate the conclusions found.

The first table describes the number of bits used by individual edges and caps in both methods. The caps of McGuire and Hughes' method uses only a small amount of memory relative to the edges because they make use of the edge data. There is also some memory used by the GLSL edges and caps not mentioned here, because it is transparently created and destroyed by the graphics pipeline. 32-bit float and integer types were assumed.

	Memory Usage Per Item
Ar Edge	640 bits
M&H Edge	2688 bits
Ar Cap	576 bits
M&H Cap	96 bits

Then, for a sample of objects, the next table compares the number of edges and caps used by both methods.

	Edges (Ar & M&H)	Caps (Ar)	Caps (M&H)	Cap:Edge Ratio (Ar)	Cap:Edge Ratio (M&H)
Cube	24	24	48	1	2
Merged Cube	12	24	24	2	2
Cylinder	96	320	192	3.33	2
Merged Cylinder	96	192	192	2	2
Cone	64	592	128	9.25	2
Quad Sphere	2016	6944	4032	3.44	2
Ico Sphere	1920	9570	3840	4.98	2
Teapot	1180	4420	2360	3.75	2
Monkey	1449	7188	2898	4.96	2
Bunny	20812	107290	41624	5.16	2

The number of caps to edges in McGuire and Hughes' method is always two because there are two half caps drawn for each edge, one on each side. For most meshes, the author's method will have far more caps because it handles every possible case.

Combining the information of the previous two tables, the number of bits needed by each type of object's edges and caps can be determined. They are displayed in the next table. Values are in bits.

	Edges (Ar)	Edges (M&H)	Caps (Ar)	Caps (M&H)
Cube	15360	64512	13824	4608
Merged Cube	7680	32256	13824	2304
Cylinder	61440	258048	184320	18432
Merged Cylinder	61440	258048	110592	18432
Cone	40960	172032	340992	12288
Quad Sphere	1290240	5419008	3999744	387072
Ico Sphere	1228800	5160960	5512320	368640
Teapot	755200	3171840	2545920	226560
Monkey	927360	3894912	4140288	278208
Bunny	13319680	55942656	61799040	3995904

Totaling all memory used by the edges and caps for each type of object under each method, the memory ratios illustrate that under the current system, most meshes use about the same memory in both methods. There are a few meshes that, under the author's method, have better memory usage (green), and one, the cone, with terrible memory usage (red). The cone's high memory usage comes from the high numbers of caps that occur at the tip where most of the edges come together, a worst-case scenario for the author's method. Non-ratio values are in bits.

	Total Ar Memory	Total M&H Memory	Memory Ratio (Ar : M&H)
Cube	29184	69120	0.422
Merged Cube	21504	34560	0.622
Cylinder	245760	276480	0.888
Merged Cylinder	172032	276480	0.622
Cone	381952	184320	2.07
Quad Sphere	5289984	5806080	0.911
Ico Sphere	6741120	5529600	1.21
Teapot	3301120	3398400	0.971
Monkey	5067648	4173120	1.21
Bunny	75118720	59938560	1.25

If McGuire and Hughes' method is implemented in OpenCL, the memory usage looks much different, with each mesh using just over half the memory of the equivalent shader version. This is possible because each cap uses 64 fewer bits of memory than the author's method caps and there are only two caps per edge. The table below illustrates the change.

	M&H (OpenCL)	M&H (Shader)	Memory Ratio (OpenCL:Shader)
Cube	39936	69120	0.577
Merged Cube	19968	34560	0.577
Cylinder	159744	276480	0.577
Merged Cylinder	159744	276480	0.577
Cone	106496	184320	0.577
Quad Sphere	3354624	5806080	0.577
Ico Sphere	3194880	5529600	0.577
Teapot	1963520	3398400	0.577
Monkey	2411136	4173120	0.577
Bunny	34631168	59938560	0.577

### 11.3. Rendered Output

Regardless of the detection and creation speed, the number of edges and caps drawn will also influence the speed. At a given view direction, the same number of edges will be generated by both methods. However, the number of drawn caps is significantly different. In McGuire and Hughes' method, the number of caps drawn is always two times the number of edges. The author's method, though more varied, consistently generates fewer caps than McGuire and Hughes' method (green). These numbers were calculated with the camera pointing at the origin and positioned at (3, 3, 3) in world-space. The meshes were at the origin, with a scale size of approximately one.

	Edges (Ar & M&H)	Caps (Ar)	Caps (M&H)	Cap:Edge Ratio (Ar)	Cap:Edge Ratio (M&H)
Cube	24	24	48	1	2
Merged Cube	12	24	24	2	2
Cylinder	130	136	260	1.04	2
Merged Cylinder	66	72	132	1.09	2
Cone	34	37	68	1.09	2
Quad Sphere	72	72	144	1	2
Ico Sphere	55	55	110	1	2
Teapot	205	228	410	1.11	2
Monkey	345	488	690	1.41	2
Bunny	1175	1397	2350	1.19	2

Using McGuire and Hughes' capping method with OpenCL, the number of drawn caps will be the same as in the shader implementation, making the cap/edge ratio for all meshes two.

### 11.4. Speed

The rendering speed for each type of mesh is significantly varied for different architectures and algorithms. The metric used to determine speed was the overall framerate with edges, caps, and the mesh being rendered each frame. Below are the results and comparisons of three setups: CPU implementation of

both algorithms, GPU implementation of both algorithms, and McGuire and Hughes' implementation in both OpenCL and shaders.

### ***CPU Implementation***

The CPU implementations have equivalent memory access speeds for both methods. Being linear, they can also take advantage of short-circuiting. In this setup, the author's method has the distinct advantage for complex meshes because it does significantly fewer operations. It also gains the similar memory access speeds and short-circuiting, which are not available in OpenCL.

	Framerate (Ar)	Framerate (M&H)	Ratio (Ar : M&H)
Cube	1135	1156	0.982
Merged Cube	1155	1180	0.979
Cylinder	1139	1182	0.964
Merged Cylinder	1126	1128	0.998
Cone	1276	1338	0.954
Quad Sphere	679	144	4.715
Ico Sphere	631	155	4.071
Teapot	906	226	4.009
Monkey	602	176	3.42
Bunny	54	14	3.857

### ***GPU Implementation***

Next, the optimized OpenCL version of the author's method is compared to the shader version of McGuire and Hughes' method. As described earlier, the reduction in total processing is less meaningful with slower memory access and a lack of short-circuiting. The shader's advantages allow McGuire and Hughes' algorithm to consistently achieve higher speeds than the author's algorithm. Further, some framerates for the OpenCL version of the author's method are actually slower on the GPU than on the CPU.

	Framerate (Ar)	Framerate (M&H)	Ratio (Ar : M&H)
Cube	760	1173	0.647
Merged Cube	768	1184	0.648
Cylinder	733	1103	0.664
Merged Cylinder	741	1142	0.648
Cone	724	1244	0.581
Quad Sphere	416	713	0.583
Ico Sphere	360	739	0.487
Teapot	464	850	0.545
Monkey	334	770	0.433
Bunny	31	134	0.231

### **McGuire and Hughes' Cap Method on both OpenCL and Shaders**

Finally, McGuire and Hughes' cap algorithm usage is compared in both OpenCL and shaders. Only for the most complex of meshes does the OpenCL method beat out the shader version in terms of speed. In the table below, "CL" refers to the OpenCL version, and "GLSL" refers to the shader version.

	Framerate (CL)	Framerate (GLSL)	Ratio (CL : GLSL)
Cube	762	1173	0.649
Merged Cube	770	1184	0.65
Cylinder	735	1103	0.666
Merged Cylinder	749	1142	0.655
Cone	670	1244	0.538
Quad Sphere	584	713	0.819
Ico Sphere	593	739	0.802
Teapot	631	850	0.742
Monkey	634	770	0.823
Bunny	159	134	1.18

## 12. Conclusion

---

The depth-based edge thickness scaling factor provides more realistic edge shapes and reduces artifacts at almost no additional cost. Badly oriented normals can be prevented using duplicate edges for crease edges. For some meshes, with observation and testing, duplicate edges can be avoided by determining which normals to use and which to ignore. The plug and half hex methods of edge creation can be used to reduce the number of render passes by one, while retaining approximately the same quality as McGuire and Hughes' method of edge and cap creation.

The author's method of capping, while initially showing promise in terms of speed, only has an advantage in terms of accuracy. OpenCL memory access speeds and a few other implementation issues severely limit its practicality for object-space edge detection. Only for very complex meshes can it be made to run faster than an equivalent shader implementation. Future improvements to OpenCL may eventually allow it to run at equivalent or faster speeds than McGuire and Hughes' shader-based method.

## 13. Future Work

---

McGuire and Hughes' paper mentions the use of geometry shaders and data texture access as a method to reduce the amount of duplicate information and calculations. These technologies are now commonly available. They might also be considered as a non-OpenCL method of implementing the author's method of capping.

If GPU data indexing is not used by the OpenCL implementation of McGuire and Hughes' method, the vertex and normal data would be duplicated once in edge-specific buffers. In that case, the data would be ordered and OpenCL could take advantage of manual data caching. This would solve the memory access speed problem at the cost of additional memory usage, but it is not known if this alone would be enough to surpass the shader implementation in terms of speed.

Microsoft's DirectCompute shaders have many of the same abilities as OpenCL and any of the discussed methods could be implemented using that technology. One advantage it has over OpenCL is the ability to export calculations to the graphics pipeline. This will allow the edge and cap rendering passes to be integrated into the computation passes. That ability to skip two render passes could speed up the framerate slightly.

Chris Peters [Peters 10] suggested a capping method that preprocessed edges so that both ends contain a "next" index. The next index points to an adjacent edge connected to the same end point on a triangle. After doing the edge compute pass, each drawable edge would be operated on twice, once for each end. At each end of each drawable edge, the next index would be used to check the next edge for its drawability. If it is drawable, a cap is formed between those two edges. If it is not drawable, the next index of the second edge is checked, and so on, until either a drawable edge is found, or the original edge is reached. If a drawable edge connects to no drawable edges, no cap is drawn. This system should theoretically give the same accuracy caps as the author's capping method, but without needing to store or check every possible combination. The

worst case number of memory accesses is  $C + 1 + \text{DATA}$ , where  $C$  is the number of connecting edges and  $\text{DATA}$  is the other drawable edge's data needed to form the cap. This technique would still use uncached GPU memory, but requires vastly fewer memory accesses. It could potentially lead to faster speeds for more complex meshes.

## Work Cited

---

- [Binge Gamer 08] Ōkami screenshot. Ōkami (Wii). 2008. Developed by Ready at Dawn. Published by Capcom. <http://www.bingegamer.net/2008/28-new-okami-wii-screenshots/>.
- [Bosch 06] Bosch, Marc ten. 2006. "Real-Time Hardware-Determined Feature Edges." [http://www.marctenbosch.com/npr\\_edges/](http://www.marctenbosch.com/npr_edges/).
- [Buchanan and Sousa 00] Buchanan, John W., and Mario C. Sousa. 2000. "The edge buffer: A data structure for easy silhouette rendering." <ftp://ftp.cs.ualberta.ca/pub/juancho/edge.pdf>.
- [Card and Mitchell 02] Card, Drew and Jason L. Mitchell. 2002. "Non-Photorealistic Rendering with Pixel and Vertex Shaders." [http://developer.amd.com/media/gpu\\_assets/ShaderX\\_NPR.pdf](http://developer.amd.com/media/gpu_assets/ShaderX_NPR.pdf).
- [Decaudin 96] Decaudin, Philippe. 1996. "Cartoon-Looking Rendering of 3D-Scenes." <http://www.antisphere.com/Research/Publis/RR-2919-en.pdf>.
- [Evans 03] Evans, Christopher. 2003. "Thick Lines for Real-Time Cel Shading." [http://www.chrisevans3d.com/tutorials/cel\\_lines/](http://www.chrisevans3d.com/tutorials/cel_lines/).
- [Evans 03] Bomb image. Evans, Christopher. 2003. "Thick Lines for Real-Time Cel Shading." [http://www.chrisevans3d.com/tutorials/cel\\_lines/](http://www.chrisevans3d.com/tutorials/cel_lines/).
- [Gooch and Gooch 01] Gooch, Bruce and Amy Gooch. 2001. "Feature Edges: Silhouettes, Boundaries, and Creases" and "Automatic Systems: Illustration (Artistic Line Drawing)." In Non-Photorealistic Rendering. 117-159. A K Peters, Ltd.
- [Gooch et al. 99] Gooch, Bruce, Peter-Pike J. Sloan, Amy Gooch, Peter Shirley, and Richard Riesenfeld. 1999. "Interactive Technical Illustration." <http://www.ppsloan.org/publications/iti99.pdf>.

- [Hall 03] Hall, Tom. 2003. "Silhouette Tracking." <http://www.bytegeistsoftware.com/various/SilhouetteTracking.pdf>.
- [Hertzmann 99] Hertzmann, Aaron. 1999. "Introduction to 3D Non-Photorealistic Rendering: Silhouettes and Outlines." <http://citeseerx.ist.psu.edu/viewdoc/download?doi=10.1.1.93.9731&rep=rep1&type=pdf>.
- [Hertzmann and Zorin 00] Hertzmann, Aaron, and Denis Zorin. 2000. "Illustrating smooth surfaces." <http://mrl.nyu.edu/~dzorin/papers/hertzmann2000iss.pdf>.
- [HIPR 00] Hypermedia Image Processing Reference (HIPR). Robert Fisher, Simon Perkins, Ashley Walker, and Erik Wolfart. 2000. <http://homepages.inf.ed.ac.uk/rbf/HIPR2/sobel.htm>, <http://homepages.inf.ed.ac.uk/rbf/HIPR2/roberts.htm>.
- [Kroon 09] Kroon, Dirk-Jan. 2009. "Numerical Optimization Of Kernel Based Image Derivatives." [http://www.k-zone.nl/Kroon\\_DerivativePaper.pdf](http://www.k-zone.nl/Kroon_DerivativePaper.pdf).
- [Lander 01] Lander, Jeff. 2001. "Images from deep in the programmer's cave." *Game Developer*. May. 23-28.
- [Li 10] Li, Xin. 2010. Personal Communication.
- [Markosian et al. 97] Markosian, Lee, Michael A. Kowalski, Samuel J. Trychin, Lubomir D. Bourdev, Daniel Goldstein, and John F. Hughes. 1997. "Real-Time Nonphotorealistic Rendering." <ftp://ftp.cs.brown.edu/pub/papers/graphics/research/sig97-npr.pdf>.
- [Marshall 01] Marshall, Carl. 2001. "Cartoon Rendering: Real-time Silhouette Edge Detection and Rendering." In *Game Programming Gems 2*, ed. Mark DeLoura. 436-443. Charles River Media, Inc.
- [McGuire and Hughes 04] McGuire, Morgan and John F. Hughes. 2004. "Hardware-Determined Feature Edges." <http://graphics.cs.williams.edu/papers/EdgesNPAR04/edges-NPAR04.pdf>.

- [McReynolds and Blythe 99] McReynolds, Tom and David Blythe. 1999. "Advanced Graphics Programming Techniques Using OpenGL." SIGGRAPH '99 Course. <http://www.opengl.org/resources/code/samples/sig99/advanced99/notes/node108.html>.
- [Next Level, The 03] Viewtiful Joe screenshot. Viewtiful Joe. 2003. Developed by Capcom Production Studio 4. Published by Capcom. [http://www.the-nextlevel.com/reviews/gamecube/viewtiful\\_joe\\_import/](http://www.the-nextlevel.com/reviews/gamecube/viewtiful_joe_import/).
- [Northrup and Markosian 00] Northrup, J.D., Lee Markosian. 2000. "Artistic Silhouettes: A Hybrid Approach." <http://graphics.cs.brown.edu/research/art/artistic-sils/artistic-sils-300dpi.pdf>.
- [Peters 10] Peters, Chris. 2010. Personal Communication.
- [Raskar 01] Raskar, Ramesh. 2001. "Hardware Support for Non-photorealistic Rendering." <http://www.cs.unc.edu/~raskar/HWWS/raskarHardwareNPR2001.pdf>.
- [Raskar and Cohen 99] Raskar, Ramesh and Michael Cohen. 1999. "Image Precision Silhouette Edges." <http://www.cs.unc.edu/~raskar/NPR/sil-i3d99.pdf>.
- [Rossignac and Emmerik 92] Rossignac, Jarek R. and Maarten van Emmerik. 1992. "Hidden contours on a frame-buffer." <http://www.gvu.gatech.edu/~jarek/papers/Hidden.pdf>.
- [Saito and Takahashi 90] Saito, Takafumi and Tokiichiro Takahashi. 1990. "Comprehensible Rendering of 3-D Shapes." ACM: Computer Graphics, Volume 24, Number 4. August. <http://citeseerx.ist.psu.edu/viewdoc/download?doi=10.1.1.83.4139&rep=rep1&type=pdf>.
- [Sander et al. 00] Sander, Pedro V., Xianfeng Gu, Steven J. Gortler, Hugues Hoppe, and John Snyder. 2000. "Silhouette Clipping." <http://research.microsoft.com/en-us/um/people/hoppe/silclip.pdf>.

## Bibliography

---

- [Aila and Miettinen 04] Aila, Timo and Ville Miettinen. "dPVS: An Occlusion Culling System for Massive Dynamic Environments." IEEE Computer Graphics and Applications, vol. 24, no. 2. 86-97. March.
- [Akenine-Möller et al. 08] Akenine-Möller, Tomas, Eric Haines, and Naty Hoffman. 2008. "Non-Photorealistic Rendering." In Real-Time Rendering, Third Edition. 507-530. A K Peters, Ltd.
- [Binge Gamer 08] Ōkami screenshot. Ōkami (Wii). 2008. Developed by Ready at Dawn. Published by Capcom. <http://www.bingegamer.net/2008/28-new-okami-wii-screenshots/>.
- [Bosch 06] Bosch, Marc ten. 2006. "Real-Time Hardware-Determined Feature Edges." [http://www.marctenbosch.com/npr\\_edges/](http://www.marctenbosch.com/npr_edges/).
- [Buchanan and Sousa 00] Buchanan, John W., and Mario C. Sousa. 2000. "The edge buffer: A data structure for easy silhouette rendering." <ftp://ftp.cs.ualberta.ca/pub/juancho/edge.pdf>.
- [Card and Mitchell 02] Card, Drew and Jason L. Mitchell. 2002. "Non-Photorealistic Rendering with Pixel and Vertex Shaders." [http://developer.amd.com/media/gpu\\_assets/ShaderX\\_NPR.pdf](http://developer.amd.com/media/gpu_assets/ShaderX_NPR.pdf).
- [Decaudin 96] Decaudin, Philippe. 1996. "Cartoon-Looking Rendering of 3D-Scenes." <http://www.antisphere.com/Research/Publis/RR-2919-en.pdf>.
- [Evans 03] Evans, Christopher. 2003. "Thick Lines for Real-Time Cel Shading." [http://www.chrisevans3d.com/tutorials/cel\\_lines/](http://www.chrisevans3d.com/tutorials/cel_lines/).
- [Evans 03] Bomb image. Evans, Christopher. 2003. "Thick Lines for Real-Time Cel Shading." [http://www.chrisevans3d.com/tutorials/cel\\_lines/](http://www.chrisevans3d.com/tutorials/cel_lines/).
- [Everitt 00] Everitt, Cass. 2000. "One-Pass Silhouette Rendering with GeForce and GeForce2." NVIDIA Corporation White Paper.

- [Gooch and Gooch 01] Gooch, Bruce and Amy Gooch. 2001. "Feature Edges: Silhouettes, Boundaries, and Creases" and "Automatic Systems: Illustration (Artistic Line Drawing)." In Non-Photorealistic Rendering. 117-159. A K Peters, Ltd.
- [Gooch et al. 99] Gooch, Bruce, Peter-Pike J. Sloan, Amy Gooch, Peter Shirley, and Richard Riesenfeld. 1999. "Interactive Technical Illustration." <http://www.ppsloan.org/publications/iti99.pdf>.
- [Hall 03] Hall, Tom. 2003. "Silhouette Tracking." <http://www.bytegeistsoftware.com/various/SilhouetteTracking.pdf>.
- [Hertzmann 99] Hertzmann, Aaron. 1999. "Introduction to 3D Non-Photorealistic Rendering: Silhouettes and Outlines." <http://citeseerx.ist.psu.edu/viewdoc/download?doi=10.1.1.93.9731&rep=rep1&type=pdf>.
- [Hertzmann and Zorin 00] Hertzmann, Aaron, and Denis Zorin. 2000. "Illustrating smooth surfaces." <http://mrl.nyu.edu/~dzorin/papers/hertzmann2000iss.pdf>.
- [HIPR 00] Hypermedia Image Processing Reference (HIPR). Robert Fisher, Simon Perkins, Ashley Walker, and Erik Wolfart. 2000. <http://homepages.inf.ed.ac.uk/rbf/HIPR2/sobel.htm>, <http://homepages.inf.ed.ac.uk/rbf/HIPR2/roberts.htm>.
- [Isenberg et al. 03] Isenberg, Tobias, Bert Freudenberg, Nick Halper, Stefan Schlechtweg, and Thomas Strothotte. 2003. "A Developer's Guide to Silhouette Algorithms for Polygonal Models." IEEE Computer Graphics and Applications, vol. 23, no. 4. 28-37. July.
- [Kroon 09] Kroon, Dirk-Jan. 2009. "Numerical Optimization Of Kernel Based Image Derivatives." [http://www.k-zone.nl/Kroon\\_DerivativePaper.pdf](http://www.k-zone.nl/Kroon_DerivativePaper.pdf).
- [Lander 01] Lander, Jeff. 2001. "Images from deep in the programmer's cave." Game Developer. May. 23-28.

- [Li 10] Li, Xin. 2010. Personal Communication.
- [Markosian et al. 97] Markosian, Lee, Michael A. Kowalski, Samuel J. Trychin, Lubomir D. Bourdev, Daniel Goldstein, and John F. Hughes. 1997. "Real-Time Nonphotorealistic Rendering." <ftp://ftp.cs.brown.edu/pub/papers/graphics/research/sig97-npr.pdf>.
- [Marshall 01] Marshall, Carl. 2001. "Cartoon Rendering: Real-time Silhouette Edge Detection and Rendering." In *Game Programming Gems 2*, ed. Mark DeLoura. 436-443. Charles River Media, Inc.
- [McGuire and Hughes 04] McGuire, Morgan and John F. Hughes. 2004. "Hardware-Determined Feature Edges." <http://graphics.cs.williams.edu/papers/EdgesNPAR04/edges-NPAR04.pdf>.
- [McReynolds and Blythe 99] McReynolds, Tom and David Blythe. 1999. "Advanced Graphics Programming Techniques Using OpenGL." SIGGRAPH '99 Course. <http://www.opengl.org/resources/code/samples/sig99/advanced99/notes/node108.html>.
- [Mitchell 02] Mitchell, Jason L. 2002. "Image Processing with 1.4 Pixel Shaders in Direct3D." [http://developer.amd.com/media/gpu\\_assets/ShaderX\\_ImageProcessing.pdf](http://developer.amd.com/media/gpu_assets/ShaderX_ImageProcessing.pdf).
- [Next Level, The 03] Viewtiful Joe screenshot. Viewtiful Joe. 2003. Developed by Capcom Production Studio 4. Published by Capcom. [http://www.the-nextlevel.com/reviews/gamecube/viewtiful\\_joe\\_import/](http://www.the-nextlevel.com/reviews/gamecube/viewtiful_joe_import/).
- [Northrup and Markosian 00] Northrup, J.D., Lee Markosian. 2000. "Artistic Silhouettes: A Hybrid Approach." <http://graphics.cs.brown.edu/research/art/artistic-sils/artistic-sils-300dpi.pdf>.
- [Peters 10] Peters, Chris. 2010. Personal Communication.
- [Raskar 01] Raskar, Ramesh. 2001. "Hardware Support for Non-photorealistic Rendering." <http://www.cs.unc.edu/~raskar/HWWS/raskarHardwareNPR2001.pdf>.

- [Raskar and Cohen 99] Raskar, Ramesh and Michael Cohen. 1999. "Image Precision Silhouette Edges." <http://www.cs.unc.edu/~raskar/NPR/sil-i3d99.pdf>.
- [Rossignac and Emmerik 92] Rossignac, Jarek R. and Maarten van Emmerik. 1992. "Hidden contours on a frame-buffer." <http://www.gvu.gatech.edu/~jarek/papers/Hidden.pdf>.
- [Saito and Takahashi 90] Saito, Takafumi and Tokiichiro Takahashi. 1990. "Comprehensible Rendering of 3-D Shapes." ACM: Computer Graphics, Volume 24, Number 4. August. <http://citeseerx.ist.psu.edu/viewdoc/download?doi=10.1.1.83.4139&rep=rep1&type=pdf>.
- [Sander et al. 00] Sander, Pedro V., Xianfeng Gu, Steven J. Gortler, Hugues Hoppe, and John Snyder. 2000. "Silhouette Clipping." <http://research.microsoft.com/en-us/um/people/hoppe/silclip.pdf>.